



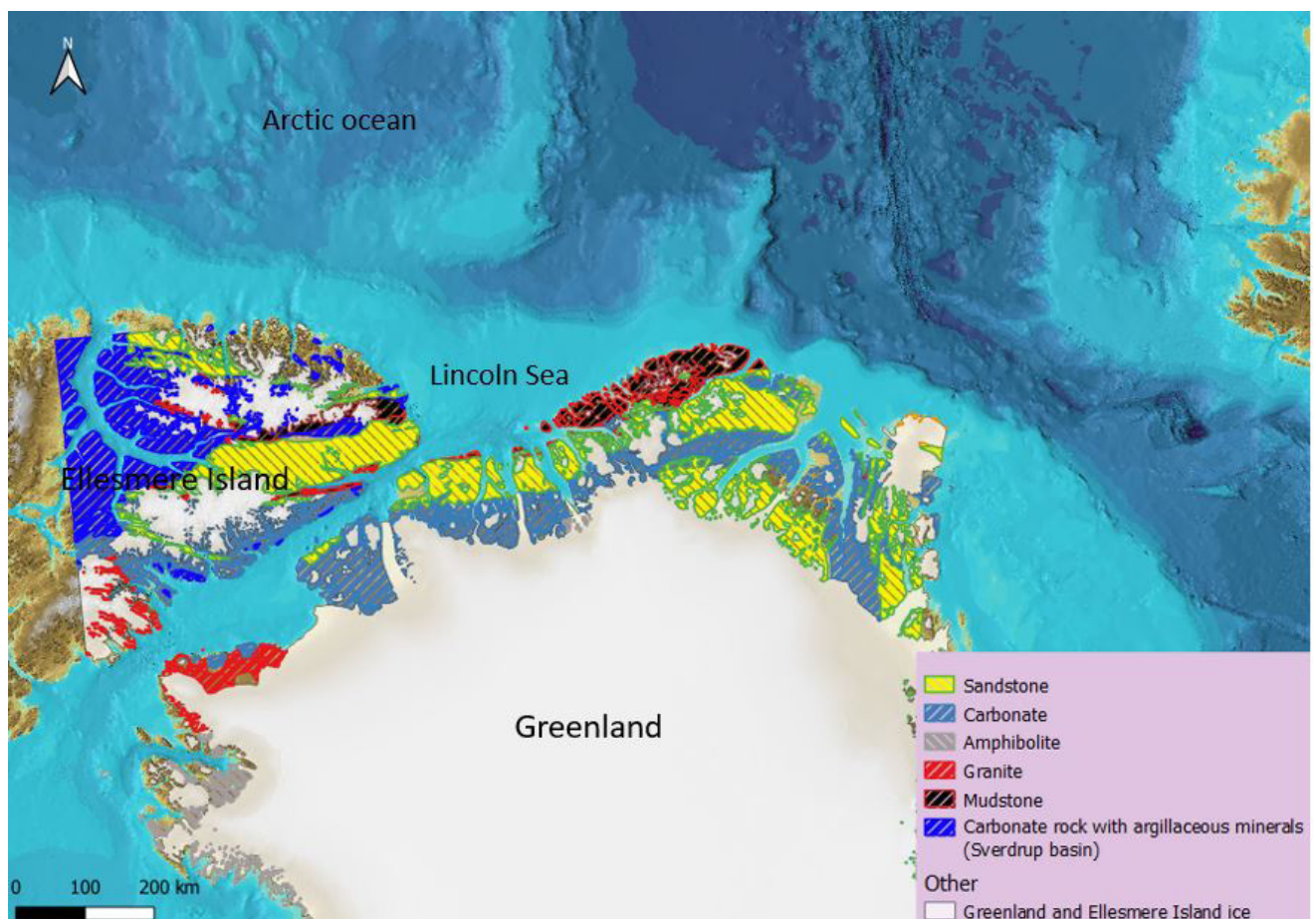
Stockholm  
University

# Master Thesis

Degree Project in  
Marine Geology 45 hp

## Clast provenance in marine diamicts from the Lincoln Sea and the Arctic Ocean and implications for deglacial ice flow patterns

Samuel Skölblom



Stockholm 2021

Department of Geological Sciences  
Stockholm University  
SE-106 91 Stockholm

# Table of Content

|   |           |
|---|-----------|
| <b>1. Abstract</b> .....  | <b>3</b>  |
| <b>2. Preface</b> .....   | <b>4</b>  |
| <b>3. Introduction</b> .....  | <b>5</b>  |
| 3.1 The modern Arctic.....  | 7         |
| 3.2 Overview of the Glacial Arctic .....                                    | 9         |
| 3.3 Northern Greenland - Innuitian and Greenland Ice Sheets movements ..... | 11        |
| <b>4. The geology of Greenland</b> .....                                    | <b>15</b> |
| 4.1 Carbonate bedrock in the Arctic .....                                   | 15        |
| 4.2 The Franklinian Basin and Ellesmere Island.....                         | 17        |
| 4.3 Formation of the Franklinian Basin.....                                 | 18        |
| 4.4 The crystalline basement of the Franklinian Basin.....                  | 19        |
| <b>5. Methods</b> .....   | <b>20</b> |
| 5.1 Processing northern Greenland samples.....                              | 21        |
| 5.2 Processing the Arctic Ocean samples.....                                | 22        |
| 5.3 Extracting Published Legacy Data.....                                   | 23        |
| <b>6. Result</b> .....  | <b>24</b> |
| 6.1 Main rock types.....  | 25        |
| 6.2 Summary of the counted rock types and abundance of each sample.....     | 28        |
| 6.3 Rock distribution comparison.....                                       | 30        |
| 6.4 The legacy data set of Phillips and Grantz (2001).....                  | 32        |
| 6.5 Statistical testing of clast compositions.....                          | 34        |
| <b>7. Discussion</b> .....  | <b>37</b> |
| 7.1 Clast composition and links to past ice flow in northern Greenland..... | 37        |
| 7.2 The sub-ice bedrock of northern Greenland.....                          | 40        |
| 7.3 Comparing clast compositions.....                                       | 42        |
| 7.4 Source of error and future work.....                                    | 43        |
| <b>8. Conclusion</b> .....  | <b>43</b> |
| <b>9. Acknowledgement</b> .....   | <b>44</b> |
| <b>10. References</b> .....   | <b>44</b> |
| <b>11. Appendix</b> .....   | <b>49</b> |

## 1. Abstract

Understanding the glacial history and the modern Arctic is not that easy but it is important. A few reasons why it is important is knowing when and how quickly the ice sheets grew and retreated but also what the ice movement direction were and were they moved to. To get a better knowledge about the glacial ice and sea ice of northern Greenland and the Arctics, analyzing ice rafted debris (rock fragments) which was dropped by icebergs flooding out to sea during the last deglaciation, can be used. However, since the Ryder expedition was the first one to enter the Lincoln Sea, this is an area we do not know much about. The carbonates that were found are quite unique for the Arctic since they are generally only found in parts of north Greenland and southeastern Ellesmere Island which makes it a good proxy for ice movement. The main rock types found in the samples from the Lincoln Sea and the Arctic Ocean besides the carbonate, are mudstone, sandstone, granite, gabbro, and amphibolite. Besides the northern Greenland samples which was divided into three qualitative groups, samples from the Central Arctic Ocean were also analyzed to compare the areas. If these rock assemblages are different, it means that icebergs have extended further out into the Central Arctic Ocean. The northern Greenland samples will also be compared with a large legacy dataset from *Phillips and Grants (2001)*. Depending on the results and besides the idea that icebergs extended further out into the Central Arctic Ocean, this comparison could also indicate that the icebergs could be traveling in the Beaufort Gyre or being trapped in the Transpolar Drift. By looking at ice flow and ice stream direction of northern Greenland and Ellesmere Island, it is clear that the ice flow of northern Greenland and the Ellesmere-Greenland Ice Shelf are heading east towards Fram Strait in eastern Greenland.

## **2. Preface**

This master's thesis has been conducted for the geological sciences at Stockholm University. The thesis covers 45 HP within the master program in geological sciences. The work was done between November 2020 – June 2021. The supervisor for the project was Matthew O Regan, associate professor in marine geology.

Stockholm University 2021

### 3. Introduction

The glacial history of the Arctic and how it impacted ocean and sea ice dynamics is important for reconstructing regional and global sea level, understanding when, why and how quickly Circum-Arctic icesheets grew and retreated (*Jakobsson et al, 2014; Batchelor et al., 2019*). Considerable uncertainty remains concerning past glacial environments even as recently as during last glacial maxima (LGM) and during the Holocene period (11.7 ka) (*Jakobsson et al, 2014*). Glacial reconstructions are often done by combining terrestrial field-based studies (the mapping and dating of glacial landforms), with mapping and dating glacial landforms on the seafloor. In deeper marine environments, sediments were deposited in front of grounded ice, and can record a signal of glacial activity on the surrounding landmasses. One of the keyways this is done is by looking at the composition of iceberg rafted sediments, which is material that was eroded by ice on land and deposited further out at sea by icebergs (*Figure 1*). The use of petrographic analyses to assess sources of glacially transported ice are referred to as clast provenance studies. Such analyses have been done by *Phillips and Grantz (2001)* conducted around the Arctic Ocean, *Caron et al (2020)* which were conducted in northwestern Greenland and Kane Basin, and *Korstgard and Nielsen (1989)* which were conducted in Baffin Bay and the Labrador Sea.

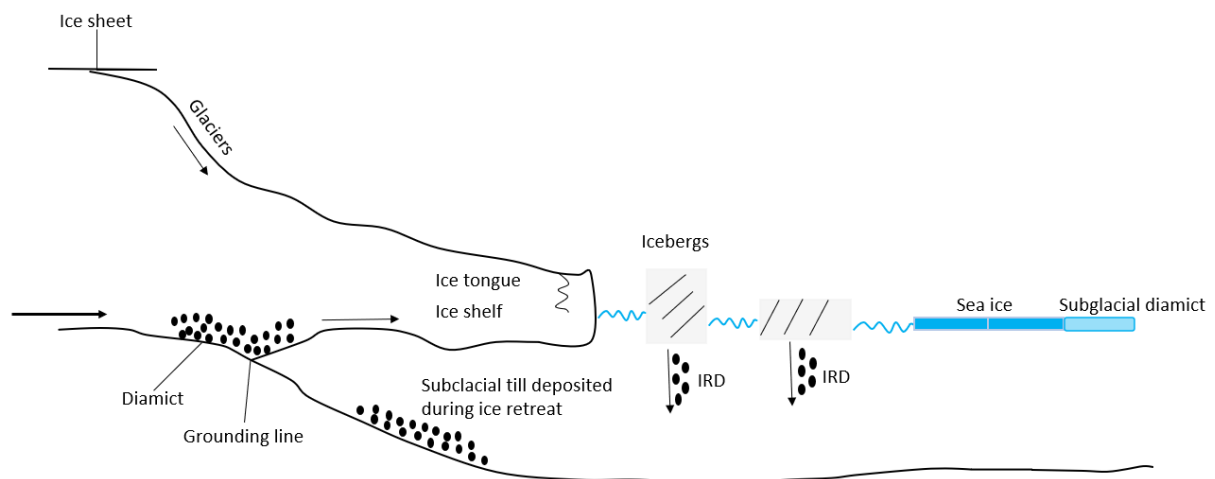


**Figure 1:** The process creating ice rafted debris (IRD) which indicates that Coarse grained IRD can be transported to sea either directly as subglacial till or grounding zone proximal diamicts, or the melting of icebergs calved from the glacier or ice tongue.

To be able to apply clast provenance studies, a basic requirement is knowledge of the geologic formations that are eroded by ice in different regions of the Arctic. Even though considerable data exists about the bedrock geology of Arctic Canada and Greenland (*Harrison et al, 2008*), there are very few studies concerning the clast composition of material transported to sea by icebergs calved in these regions. The Laurentide, Inuitian- and Greenland Ice Sheet are particularly important for the glacial reconstruction of the northern hemisphere since these three ice sheets constitutes a large part of the northern hemisphere glacial ice mass. The northern margin of these ice sheets border some of the most heavily sea ice covered waters in the Arctic Ocean, which makes access to marine records difficult.

The 2019 Ryder Expedition on icebreaker Oden was the first time a research vessel entered into the Lincoln Sea and Sherard Osborn Fjord (*Figure 2*). Due to the lack of previous marine geological studies, this is an area where we do not know much about the offshore limits and dynamics of ice sheets, ice streams and ice shelves. The main idea of this study is to reconstruct the provenance of clast material by looking at different size fractions recovered in basal diamicts from sediment cores

collected on the Ryder Expedition, and use this to investigate the origin and flow direction of the glacial ice that deposited it. The aims of the project are to 1) determine the composition and variability of ice rafted clasts along the northern Greenland coast, 2) assess whether they can be used to constrain deglacial ice flow patterns, and 3) evaluate whether the clast composition from this region of the Arctic is unique and can be used to identify the provenance of ice rafted material in distal sediment records from the Arctic.

Samples from Petermann Fjord, the Lincoln Sea, and the Sherard Osborn Fjord (*Figure 2*) are compared with clast assemblages from marine sediment cores from the Central Arctic. This was done to assess whether the Lincoln Sea had a characteristic clast assemblage that could be used as a provenance indicator in sediment cores from across the Arctic. This includes new analyses of eight sediment cores from the southern Lomonosov Ridge and the Morris Jessup Rise, as well as digitizing and large legacy dataset on Circum-Arctic clast composition published by *Phillips and Grantz (2001)*.

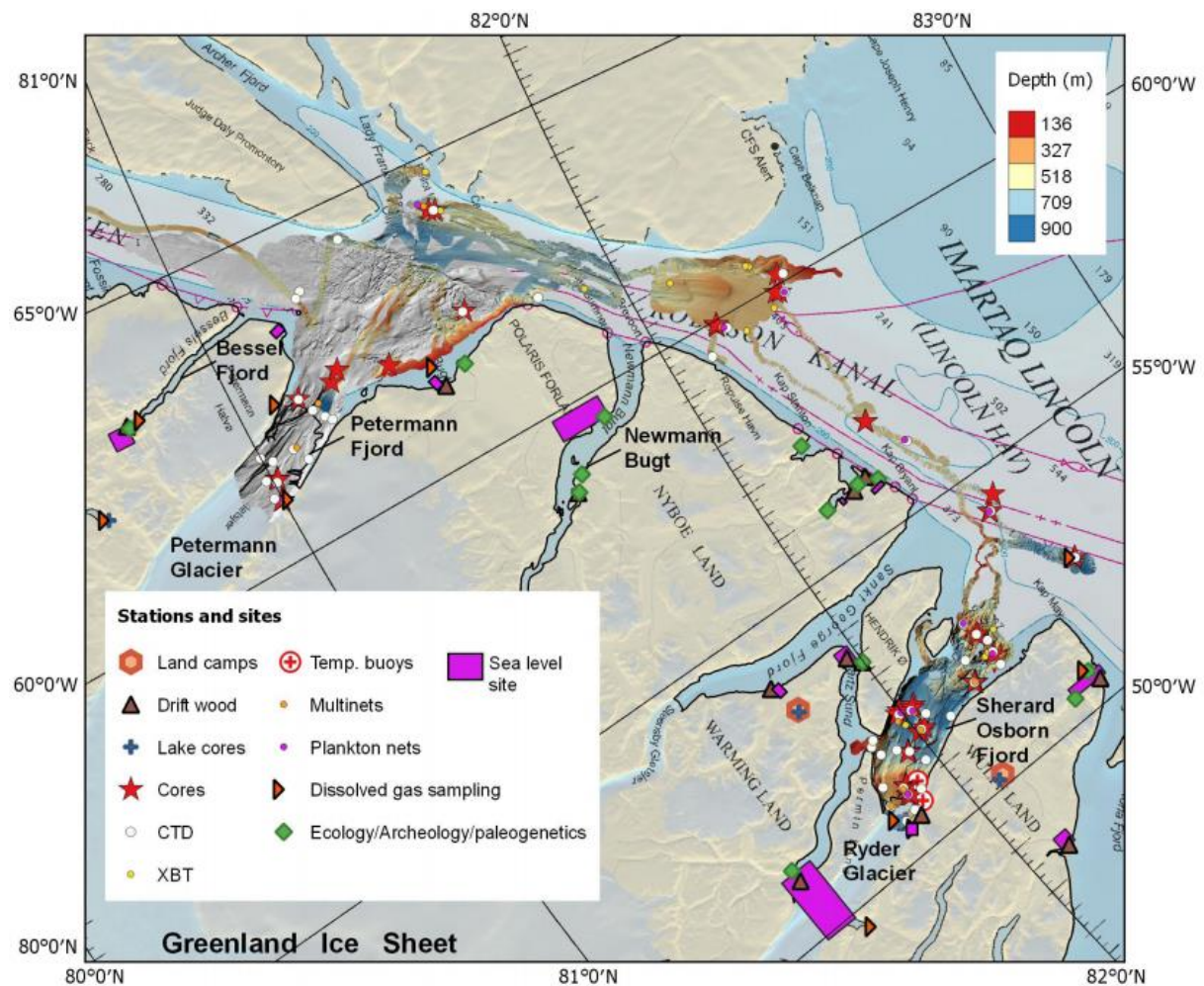


**Figure 2:** Overview map of the target regions for the Ryder 2019 expedition in the northern Greenland area which are the Petermann Fjord, Lincoln Sea and Sherard Osborn Fjord. The map also shows the acquired multibeam bathymetry (colored by depth) (Ryder expedition report, Jakobsson et al, 2019).

### 3.1 The Modern Arctic

One of the major water masses in the Arctic today is the Atlantic water layer which is found at the depth between 200-800 m (Shu et al, 2019). This water enters through the Fram Strait and across the shallow Barents -and Kara Sea. It then circulates counterclockwise around the Arctic, crossing the northern Greenland margin before returning to the Norwegian Greenland Sea. The modern Arctic is covered by perennial sea ice, which moves around the Arctic in two major surface circulation patterns (yellow arrows in figure 3). There wind driven surface circulation systems are the Transpolar Drift and the Beaufort Gyre. The Transpolar Drift travels from the East Siberian Sea and the Laptev Sea and then across to the Fram Strait, between Svalbard and Greenland where it exports sea ice into the Norwegian Greenland Sea (figure 3) (Jakobsson et al, 2014). In the Beaufort Gyre, sea ice can circulate for many decades before leaving the Beaufort Gyre (Bischof and Darby, 1997). Today, the sea ice thickness of the Beaufort Gyre is between 2-3 m (Figure 3). The least thick sea ice around the Arctic today is generally found along the coasts of the Eurasian margin. The thickness in these areas is as low as 0-1 m thick. The thickest sea ice in the Arctic is found around the northern coast of the Canadian Arctic Archipelago and the northern coast of Greenland where it is around 4-5 m thick (figure 3) (Perovich et al, 2020).

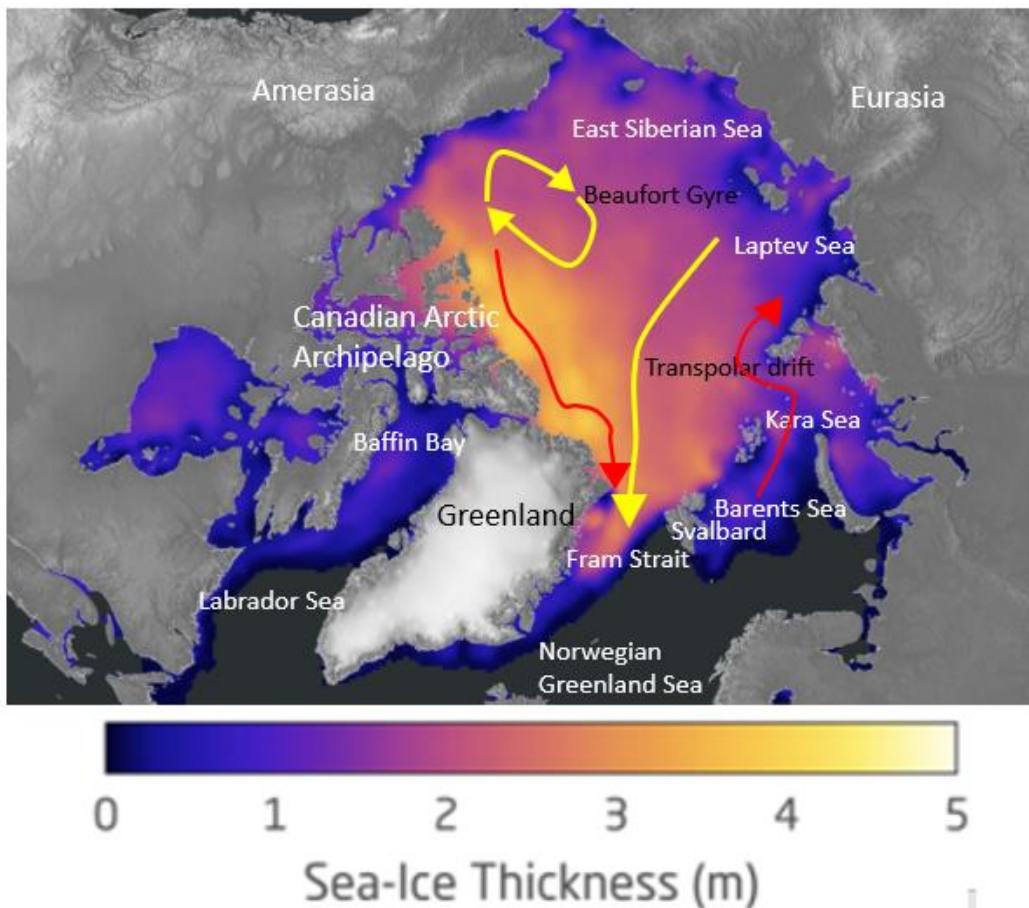


**Figure 3:** Sea ice thickness of the Arctic (in April 2020) with the sea ice drift (Transpolar Drift) the Beaufort Gyre Ocean current and water circulation in the northern Greenland (Modified from Perovich et al, 2020).

There are four important glaciers found on the coast of the northern Greenland. These glaciers are the Humboldt Glacier, Petermann Glacier, the Ryder Glacier, and the C.H. Ostenfeld Glacier (Figure 4). Humboldt Glacier is the widest outlet glacier in Greenland. This glacier terminus (end of the glacier) is thought to be grounded (ice contained in frozen ground) but the glacier also has some visible floating sections which is generally found along its northern margin (Higgins, 1989). Rignot et al (2001) synthesized that the Humboldt Glacier ice has been retreating since the early 1990's. Heavy acceleration increases of the glacier occurred in 1999 though according to Box and Decker (2011). The Petermann Glacier is one of the most studied glaciers in northern Greenland with a 21 km wide terminus in the north (Johannessen, 2013). Petermann is one of three glaciers in north Greenland that still has a generally large floating ice tongue. One time during heavy glaciation, the length of the Petermann ice tongue was as long as 70 km (Rignot et al 2001). However, due to ice retreat, the ice tongue has decreased to only 48 km in length (Hill et al, 2017). In the north of the glacier, the Petermann Trough is found which indicates that a larger fast-flowing ice stream existed here in the past (Joughin et al, 1999).

Ryder Glacier occupies Sherard Osborn Fjord, and this glacier is about 10 km wide. The floating ice tongue of Ryder Glacier is today 29 km long. This glacier has a high discharge at its terminus of  $0.66 \text{ km}^3 \text{ a}^{-1}$ . Because of the high discharge, it is one of the most important glaciers in northern Greenland (Higgins, 1991B). Observations from explorers in the early 1900s indicates that the Ryder ice tongue extended to the mouth of Sherard Osborn Fjord but then later retreated back in mid-1950's (Davies and Krinsley, 1962). Ice retreat of the Ryder ice tongue occurred between 1992-1996 and 2006/2007 while ice extension occurred between 2002-2006 and 2007-2010 (Box and Decker, 2011). When the ice retreated, thinning occurred. If the thinning of the ice is continuing, ice retreat would keep on happening which would lead to more ice loss (Thomas et al, 2009). The C. H. Ostenfeld Glacier is generally 7-9 km wide and occupies southern parts of the Victoria Fjord. This glacier has a remarkably high ice discharge (Rignot et al 2001). The glacier ice tongue extended about 25 km from the grounding line in the end of the 1970's. The ice tongue today is still floating but it is only 1.5 km long (Higgins, 1991B).



**Figure 4:** Satellite view of north Greenland and Ellesmere Island from 2019. The velocities of the major glaciers are also shown on the map. KB=Kane Basin; HB=Hall Basin; RC=Robeson Channel (O'Regan et al, 2021).

### 3.2 Overview of the Glacial Arctic

The glacial history of the Arctic has been pieced together by combining terrestrial and marine mapping with studies of marine sediment cores. Today, Greenland is the only continental scale ice sheet in the Northern hemisphere. Analogous to the Antarctica Ice Sheet, but considerably smaller. Away from Greenland, glacial ice in the Arctic is limited to more local ice caps. Many of these are drained from relatively fast flowing marine terminating glaciers. However, the situation was much different during Pleistocene glacial periods (*Jakobsson et al, 2014*). During Quaternary glacial cycles, extensive ice caps developed over much of North America and Eurasia, while the Greenland Ice Sheet extended out onto the continental margin. Large ice shelves developed along the margins of the ice sheets and extended far out into the Arctic Ocean and were accompanied by thicker and more persistent sea ice cover (*figure 5*). These three things are particularly important for the Arctic history (*Donn & Ewing, 1966*).

The landforms found around the northern Barents -and the Kara Sea were formed in subglacial and glaciomarine environments. In northwest of Svalbard, streamlined sedimentary landforms are found in the larger fjords in the area. The streamlined sedimentary landforms give an indication of the past ice stream flow that occurred during the last glacial period. These streamlined landforms are also found in other parts of the Barents -and Kara Sea area (*Ottesen et al, 2007*). Ridges of transverse and morainic type are also common in shallow banks in the Barents -and the Kara Sea (*Kleiber et al, 2000*). Glaciations over this area are believed to have started around 3.5-2.4 Ma ago which was during the Pliocene-Pleistocene era (*Knies et al, 2009*). Between 2.6 -1.0 Ma, the glaciation increased in power which made the glaciers more land based than marine based. Around 2.3 Ma ago, the glaciers started to spread over larger areas (*Butt et al, 2002*).

The Arctic history from the Laptev Sea, and the East Siberian Sea are rather poorly investigated and only a few parts of those locations have been explored. However, marine mapping on the Arlis Plateau and the east Siberian Sea shows that parts of the East Siberian Sea contain signs that the area had been glaciated in the past (*Niessen et al, 2013; O'Regan et al, 2017*). It is believed that the glacial landforms mapped in these areas come from thick coherent ice shelves and larger ice sheets that covered the continental shelf during pre-LGM glaciations (*Wetterich et al, 2011*). In the Laptev Sea, the glacial conditions during the LGM were not the same as in and around the Siberian Sea. In the Laptev Sea, permafrost records instead give an idea of ice-free conditions (*Boucsein et al, 2002*). Glacial landforms found in and around the Chukchi margin are generally associated with iceberg plough marks (*Jakobsson et al, 2008*). In this area, there has also been indications on a sharp increase of iceberg rafted material in the middle of the Pleistocene (*Polyak et al, 2009*).

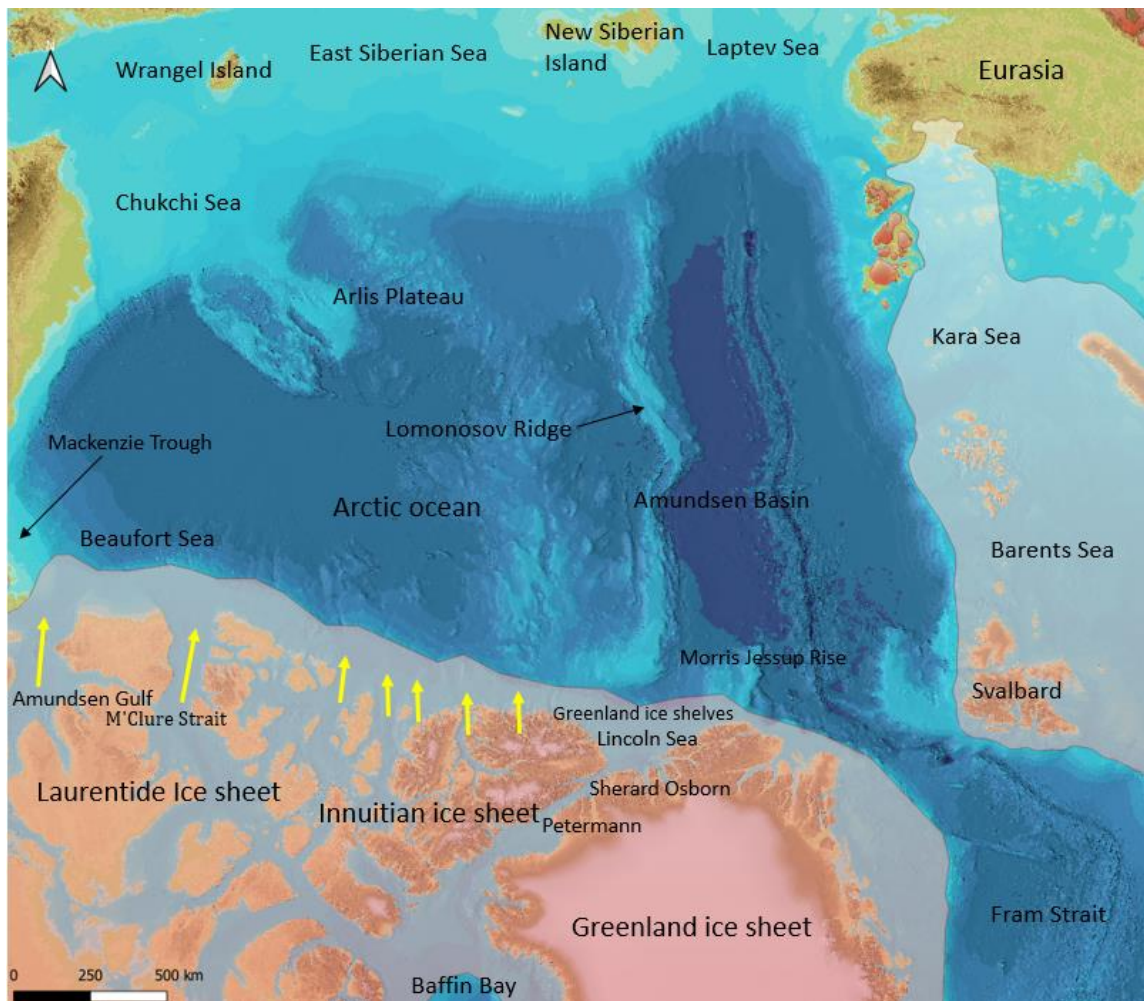


**Figure 5:** The white shaded areas indicate the ice cover during peak glacial periods during the last ice age. Major ice through (major ice streams locations in yellow arrow) of the Arctic is also shown. The map was created by GIS using IBCAO (Jakobsson et al, 2020).

Seven major ice streams fed directly into the Arctic Ocean along the Canadian Arctic coastline (Figure 5). Those ice streams came from the Laurentide and the Innuitian ice sheets that extended to the edge of the continental margin during the LGM. Around the Beaufort Sea shelf, three large glacial troughs exist, the Mackenzie Trough, M'Clure Strait, and the Amundsen Gulf (figure 5) (Stokes et al, 2005; Bischof and Darby, 1997). The active ice streams found in M'Clure Strait and Amundsen Gulf indicate that glacial ice existed to the north and south of the Banks Island (Dyke & Prest, 1987; Dyke et al, 2002). In Northern Greenland, bordering the Lincoln Sea, terrestrial mapping has shown that glacial ice extended offshore (Jakobsson et al, 2014). However, the marine realm of this continental margin has not been explored due to unbelievably harsh sea ice conditions which prevent access by marine research vessels. Terrestrial studies from the northern most coastal area of northern Greenland (Lincoln Sea) are the main source on how far the ice extended towards the Arctic Ocean. Mapping of glacial erratics, and glacial landforms, and paleo-shorelines on the coast of the northern Greenland show that a large ice cap developed over the northern Greenland mountain range. This occurred during the LGM and the ice cap that was developed was then called "The North Cap" (figure 6A and figure 6B) (Funder et al, 2011).

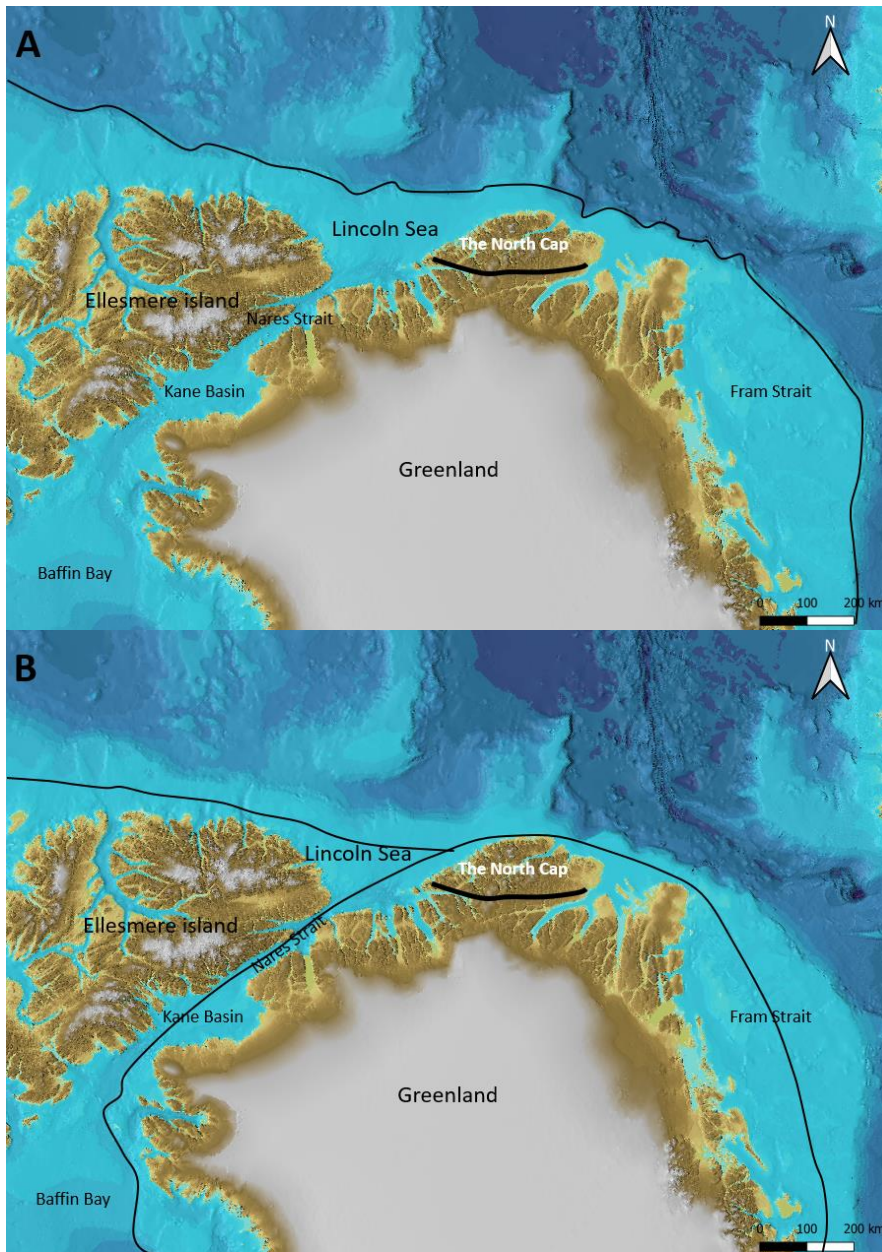


**Figure 6:** The maximum extended ice during LGM (**6A**) and the maximum extended ice during the end of the last glaciation (**6B**). The North Cap is included.

### 3.3 Northern Greenland - Innuitian and Greenland Ice Sheets movements

The configuration of glacial ice in Nares Strait during the LGM is highly debated because it is a complex area where the Innuitian and Greenland ice sheets merged together. *England and Bradley (1978)* hypothesized that the Innuitian ice sheets flowed across the Hazen Plateau, which is found on Ellesmere Island. However, some sources say that it cannot be possible due to erratics around the Hazen Plateau which shows that the ice never moved more than 20 km inland. Mapping of erratics in the northeast of Ellesmere Island confirms that the Greenland ice never crossed Hazen Plateau (*England and Bradley, 1978*). Nares strait, which is located south of the Hazen Plateau, was crossed by ice sheets going both southward and northward. It is however unclear when these ice sheets crossed the Nares Strait. One hypothesis was that the Innuitian Ice Sheet occupied the Queen Elizabeth Islands when it coalesced with the Laurentide Ice Sheet to the west and the Greenland Ice Sheet to the east and the ice moved in the same direction (*figure 7A*) (*Blake, 1992*). A second

hypothesis argued that the Queen Elizabeth Islands were occupied by ice caps that were disconnected from the Laurentide and the Greenland Ice Sheet in the way that ice did not move in the same direction (*figure 7B*). The ice caps on the Queen Elizabeth Islands were called the Franklin Ice Complex (*England, 1976*). The bedrock beneath the Franklin Ice Complex generally contains a lot of gneiss, granitoids, monzonites and different metasedimentary rocks like quartzite. The complex also contains massive greenstone belts (*Dyke et al, 1982*) which is basically metamorphosed mafic to ultramafic volcanic sequences. They are usually found within Archean cratons (stable part of the continental lithosphere) between gneiss and granite bodies (*Condie, 1981*).

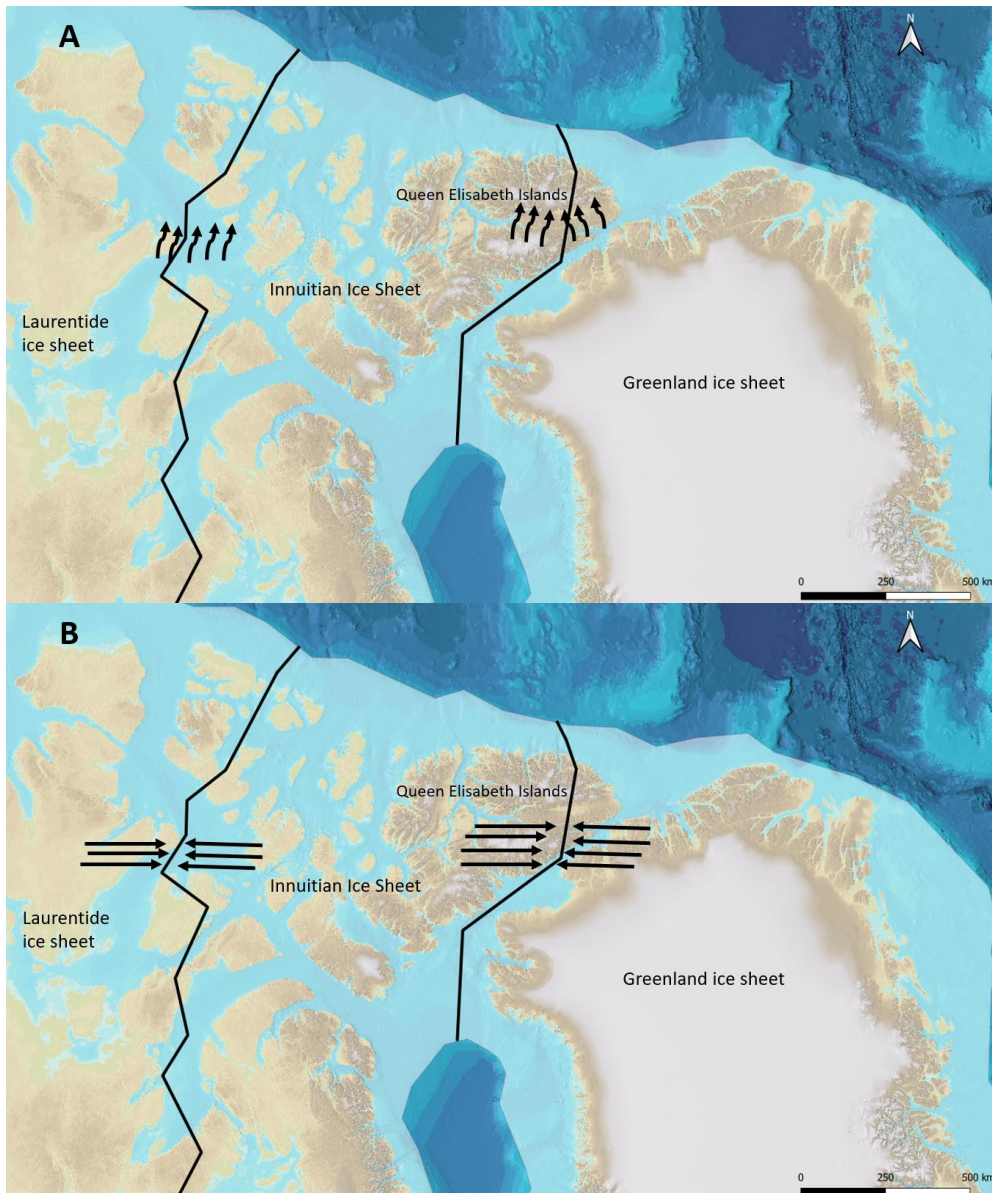


**Figure 7:** First hypothesis, were the Laurentide, Innuitian – and the Greenland Ice Sheet coalesced and ice movement in the same direction are modeled in **7A**. The second hypothesis were Innuitian Ice Sheet was disconnected from the Laurentide - and the Greenland Ice Sheet and did not move in the same direction are modeled in **7B**.

Three different observations were used to support the configuration of the Innuitian Ice Sheet during the LGM (*in figure 7A*). The first observation was that an axis of greater postglacial emergence, named the Innuitian uplift, extended from Bathurst Island to Eureka Sound (*figure 8*). The Innuitian uplift was used to determine the former maximum thickness of the Innuitian Ice Sheet which could

then be used to determine the ice configuration in the region. Lower ice thickness indicates that ice has retreated from the area and higher ice thickness indicates that ice has extended to an area (Blake, 1970). The second observation was based on the regional distribution of radiocarbon dates on marine shells, indicating that the oldest shells occur on the western part of the Queen Elizabeth Islands and the youngest in Eureka Sound. This implied that the Innuitian Ice Sheet retreated towards the Eureka Sound from the western Queen Elizabeth Island (figure 8) (England, 1999). The third and last observation was from evidence of glacial abrasion (which is basically the surface wear achieved when subglacial sediment slides or glides over bedrock) which mainly occurred along the southeast coast of Ellesmere Island. When the Innuitian Ice Sheet and Greenland Ice Sheet merged together Smith Sound Ice Stream was formed and moved from southern Nares Strait into Baffin Bay (figure 8) (Blake, 1992).

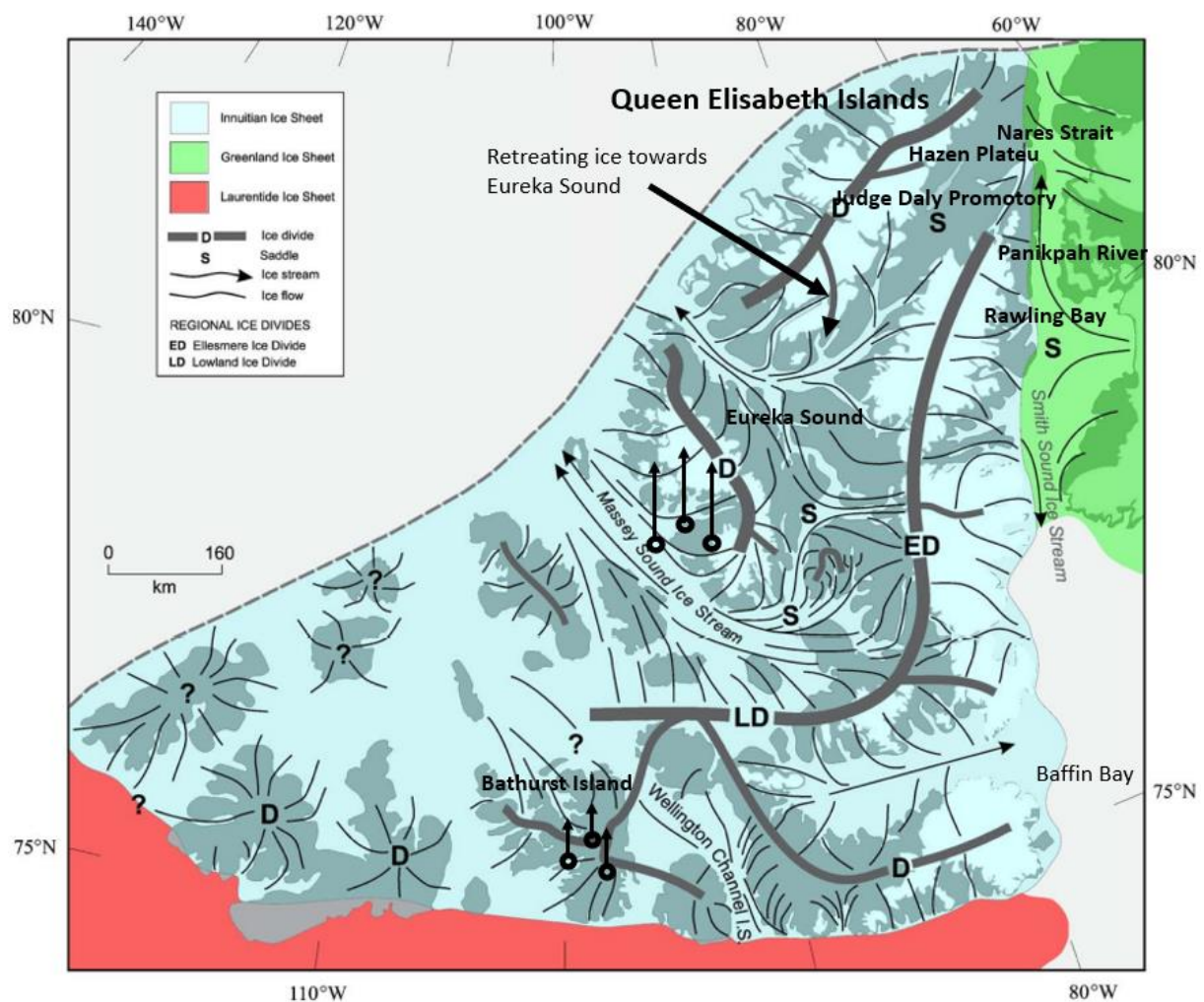


**Figure 8:** Innuitian uplift, exceeding from Bathurst Island to Eureka Sound. Stronger uplift in the eastern Innuitian Ice Sheet. The ice from the western Queen Elizabeth Island retreating towards the Eureka Sound and the Smith Sound Ice Stream heading towards and out in the Baffin Bay. The Innuitian uplift (black rings with arrow) is also shown (Modified from England et al, 2006).

The ice of Greenland and the ice of Ellesmere Island did have contact with each other which is possible to be seen on the west side of the Nares Strait, moving from north to south. The reason why it is possible to see that they were once connected to each other is because the opposing meltwater channels meet at the merged margins of the ice sheets (England, 1999). The contact between these two ice sheets indicates that the Greenland Ice Sheet once dominated parts of the Judge Daly Promontory. The Greenland ice therefore had advanced a few kilometers onto Ellesmere Island. The

Panikpah Valley of Ellesmere Island was however absent of Greenland ice. Around 60 kilometers south of the Panikpah River there is almost no Greenland ice meltwater channels. It is instead Ellesmere Island ice at this area (*England, 1999*). The contact between the Greenland ice and the Ellesmere Island ice ended around 20 km north of the Rawling Bay (which is found to the west of Nares Strait), which means that Greenland ice did not advance further than that. At the southern parts of Nares Strait, Greenland ice dominated the Smith Sound Ice Stream that was moving towards northern Baffin Bay (*figure 8*). (*England, 1999*).

On the eastern side of northern Greenland, streamlined subglacial bedforms at land occurred. These bedforms indicated a faster flowing ice stream that occupied the eastern northern Greenland in close of the Ryder Glacier and Victoria Glacier (*Funder et al, 2011*). According to *Evans et al (2009)*, large amounts of terrestrial debris flows exist in the sedimentary record along the continental slope and are compatible with the proposed extension of glacial ice to the continental shelf break (*Funder et al, 2011*).

According to *Koch (1923)*, the Greenland Ice Sheet never reached the northern coast of Greenland during the LGM. The reason for this was because of ice tongues starting to extend to the northern areas of Greenland from the North Cap (*Larsen et al, 2010*). *Funder and Larsen (1982)* suggested that the ice tongues from the North Cap, were deflected towards the east of Greenland by an ice stream occurring from the Greenland Ice Sheet. This hypothesis was generally based on occurrences of glacial erratic coming from Kap Washington to the west of the North Cap (*figure 9*). *Dawes (1986)* gave the idea that the deflected ice tongues (outlet glaciers) was caused by a large ice shelf emarging and extending from both the coasts of Greenland and Ellesmere Island (*figure 9*). This ice shelf is called the Ellesmere-Greenland Ice Shelf. The reason for the massive extension of the Ellesmere-Greenland Ice Shelf was because the ice shelf was joined by ice, mainly coming from the Nares Strait to the west, when the Greenland -and the Innuitian Ice Sheet merged together (*Funder and Hansen, 1996*). This hypothesis was later revoked. However, with new results comes new findings. The new results supported the idea that thick ice streams traveled to the north of Greenland and then merged with the ice shelf which made the ice shelf to extend even further. These results was also supported by isostatic uplift of the ice (*Funder et al., 2004*).

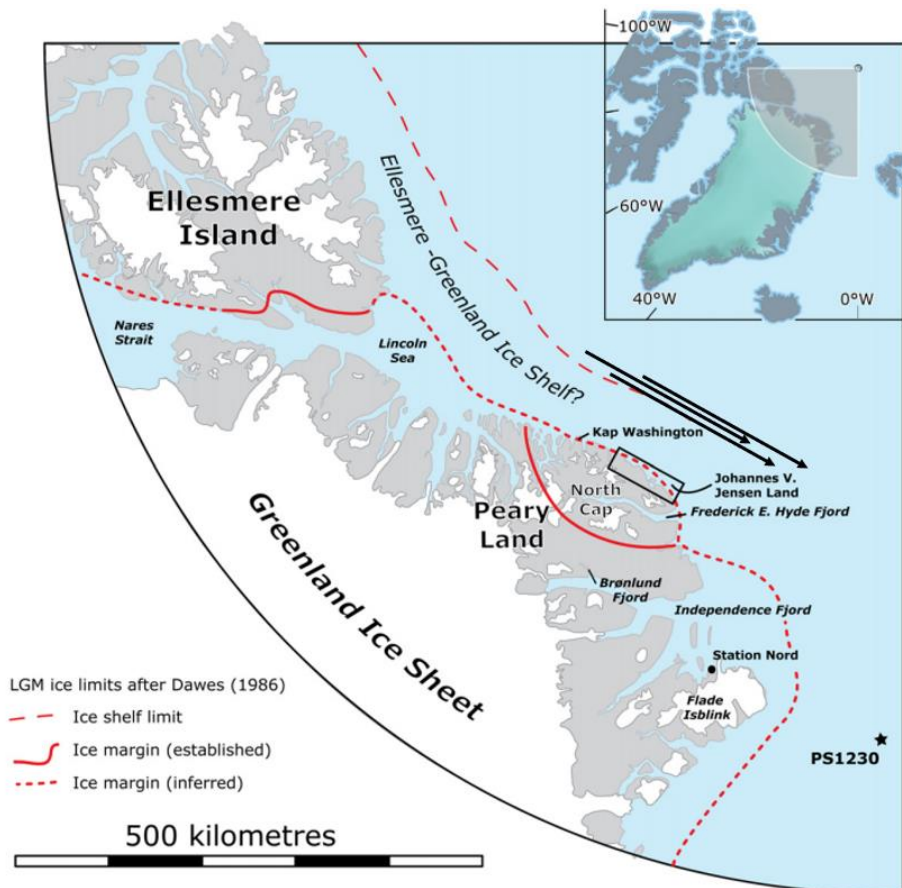


**Figure 9:** An overview map of North Greenland with LGM ice reconstructions including the deflection of the outlet glaciers (black arrows) (modified From Larsen et al, 2010).

## 4. The geology of Greenland

### 4.1 Carbonate bedrock in the Arctic

Carbonate bedrock is scarce in the Arctic and can only be found in a few regions. Usually, they are associated with formations that extend across much of the inner Canadian Arctic Archipelago and into the Mackenzie River corridor and Alaskan Beaufort Sea coast (figure 10B) (Fagel et al, 2014). Although carbonate bedrock in Canada is widely recognized, in much of the literature, there is a tendency to overlook the existence of carbonate rocks along the north Greenland coast (figure 10A). Carbonate bedrock can also be found in the south-eastern part of Ellesmere Island (figure 10A). Due to their limited distribution, carbonate rich IRD is commonly used as an indication that glacial ice was active in northern Canada (Laurentide Ice Sheet) or around the coast of northern Greenland (Greenland Ice Sheet) (Peck et al, 2007). The carbonate rock found on the northern Greenland coast are limestone and dolomite.

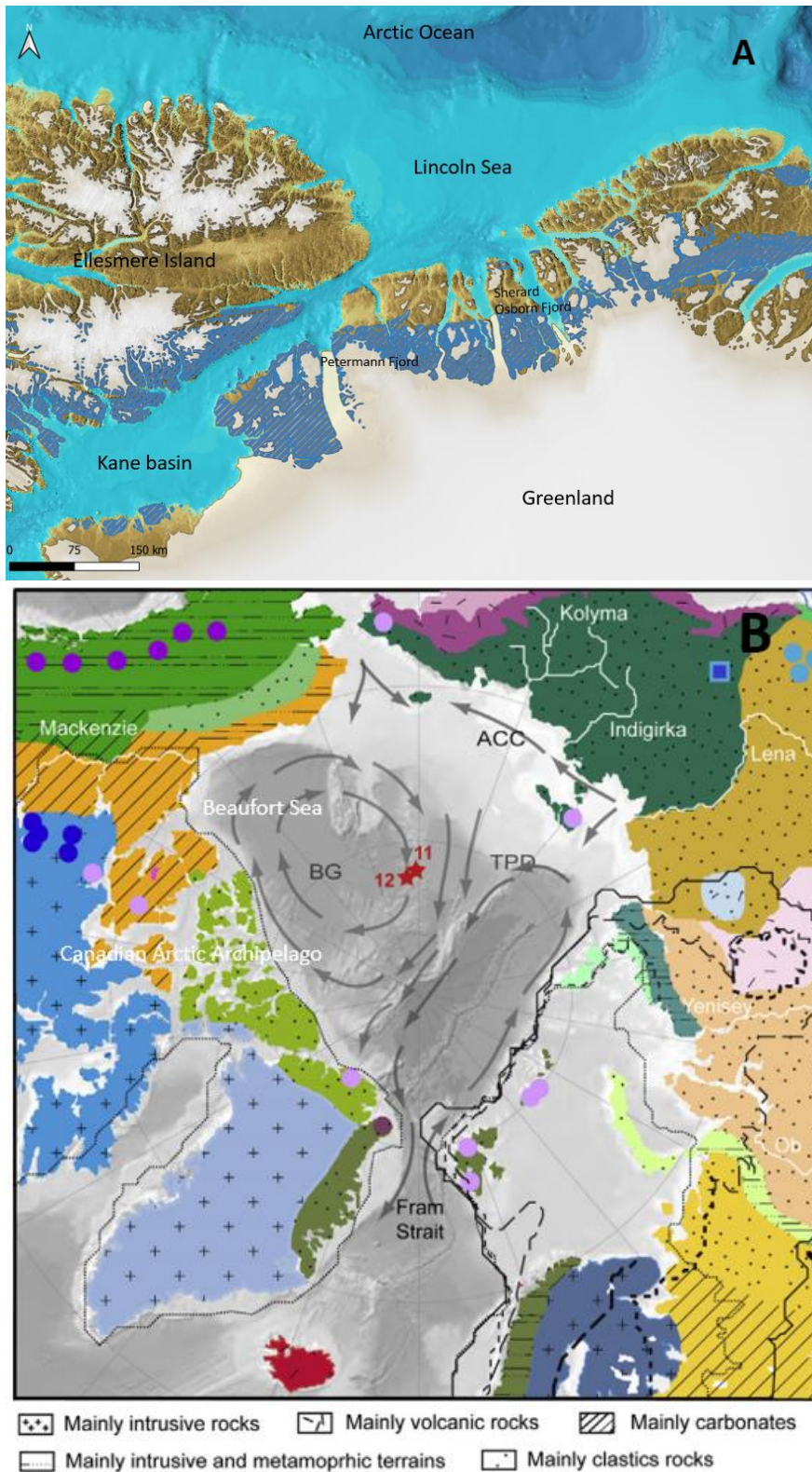


**Figure 10:** Along the top (**10A**) are the rock distribution from northern Greenland (Henriksen et al, 2009). This map was created using shapefiles for the bedrock geology of Greenland/Ellesmere Island in GIS to show the different type of bedrock found in the areas. The scale for the bedrock shapefiles was 1:2500k. Below (**10B**) is a generalized compilation of the Circum-Arctic bedrock (modified from Fagel et al, 2014).

## 4.2 The Franklinian Basin and Ellesmere Island

The Geology of the northern Greenland coast generally goes from older limestone and dolomites deposited on carbonate rimmed shelf, to younger, deeper water sandstone and mudstones deposited as turbidites on the outer continental slope. The central parts of northern Greenland and closer to the Lincoln Sea mainly consists of sandstone and siltstone but some mudstone can also be found. Not much igneous rock can be found on the surface of north Greenland, but they are instead forming the crystalline basement that is found beneath the modern ice sheet. Limited outcrops of gneiss/granite and amphibolite rock are found in the western part of north Greenland (*figure 11*). The siliclastic and carbonate rocks of northern Greenland belong to the Franklinian Basin, an ancient passive margin depositional setting.

The same siliclastic facies are found on the south-eastern parts of Ellesmere Island. The more central parts of the Ellesmere Island contain a lot of sandstone and siltstone. No or little limestone and dolomite can be found in the northern and the eastern parts of the Ellesmere Island. Igneous rocks like granite and gabbro are found beneath the surface in Arctic Canada, just like in northern Greenland. A major part of Ellesmere Island is the Sverdrup Basin. This basin is generally made up of carbonate rocks and argillaceous basin deposits which contain a large abundance of clay (*figure 11*) (*Embry & Beauchamp, 2008*). Another massive part of the Ellesmere Island is the Pearya region in northern Ellesmere Island (*figure 11*). This region is generally made up of sedimentary and volcanic rocks but also contain some amphibolite's (*Trettin, 2011*).

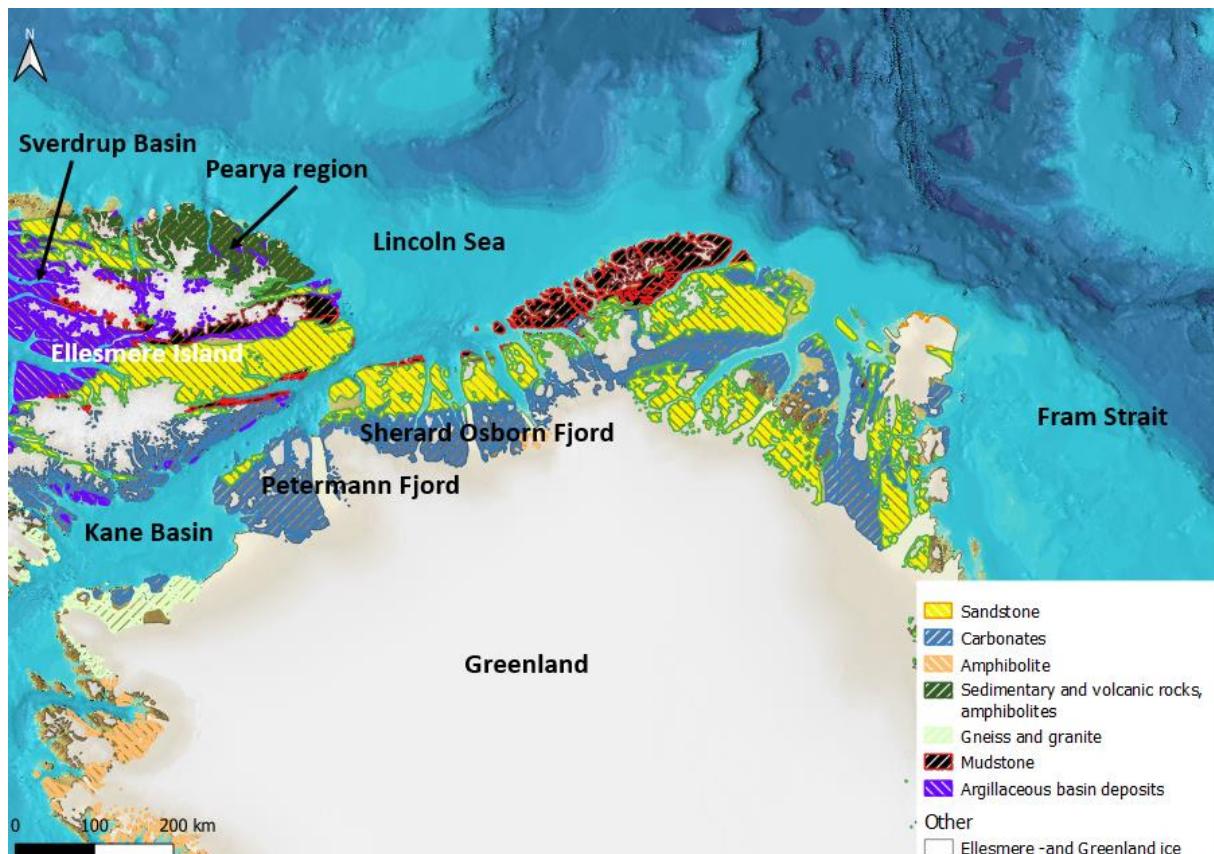


**Figure 11:** Simplified bedrock map of the northern Greenland and parts of Ellesmere Island showing the major rock types in the region.

### 4.3 Formation of the Franklinian Basin

The Franklinian Basin is found in the northern parts of Greenland and is of early Paleozoic age. The basin represents a carbonate rimmed passive margin (figure 12) (Peel and S nderholm, 1991). The Franklinian Basin was formed during seven different formation stages (Henriksen & Higgins, 2000).

In stage one, the oldest sediments were deposited. These are generally made up of dolomitic and siliciclastic sediments deposited in a marine shelf environment. These sediments are known as the Skagen group and are of early Cambrian age (Higgins et al. 1991A). This group has a limited occurrence in the northern Franklinian Basin and are only found in specific areas (Friderichsen et al. 1982). Stage two contains poorly fossiliferous dolomitic sediments. In the south of the Franklinian Basin, these sediments are generally found lying on the crystalline basement or on Proterozoic sediments like the Vendian tillites (sedimentary rocks that consist of unconsolidated masses of unweathered blocks and glacial till). The main rock type found during this stage is dolomite (Surlyk & Ineson, 1987). In stage three, sandstones, and mudstones with limited occurrences of carbonate were deposited (Soper & Higgins, 1987). This occurred due to sea-level rise which transgressed the carbonate rimmed shelf. These rocks are believed to be of late early Cambrian age (Morris et al, 1987).

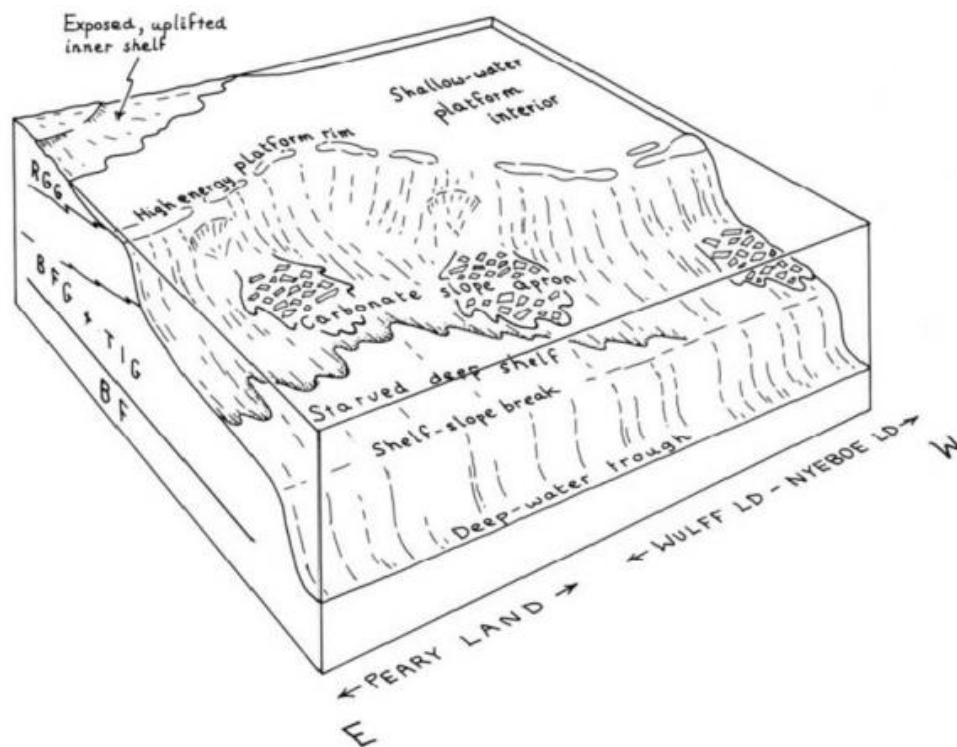


**Figure 12:** Carbonate rimmed passive margin were the Franklinian basin was formed. Deep water through on the bottom of the passive margin, carbonate slope apron and a high energy platform rim is included (Ineson & Surlyk, 1995).

The main rock types that were deposited during stage four and stage five were carbonates sequences (figure 13). The carbonate was deposited on a shelf known as the Ordovician shelf. Both limestone and dolomites are found during stage four (Bryant & Smith, 1990). The deposition of these rock types can be linked to the uplift of the northeastern Greenland (Surlyk and Hurst, 1984). In stage six, sedimentation in the Franklinian Basin changed due to the heavy uplift in eastern Greenland and erosion of denudation products (Hurst et al, 1983). Rapid deposition of turbidites started to occur along the slope and in deeper water settings. The turbidites are dated to the late Llandovery time

(early Silurian period) (Higgins & Soper, 1985).

Stage seven occurred in the later parts of the Llandovery. In this stage, the main rock types are mudstone - and siltstone turbidities interbedded with conglomerates. Between the late Llandovery to early Ludlow time (late Silurian period), a major sea-level rise occurred. The interbedded conglomerates are believed to come from high density turbidity currents (Larsen & Escher, 1987). In stage seven, the Ellesmerian Orogeny (also known as Innuitian Orogeny) also formed. No one knows for sure, but the orogeny is believed to have an age between early Devonian (which is the youngest sediments of the Franklinian Basin) and the Late Carboniferous 312 Ma (oldest post Ellesmerian deposits). The age of the orogeny on Ellesmere Island are believed to be between late Devonian to early Carboniferous age (Trettin, 1991).

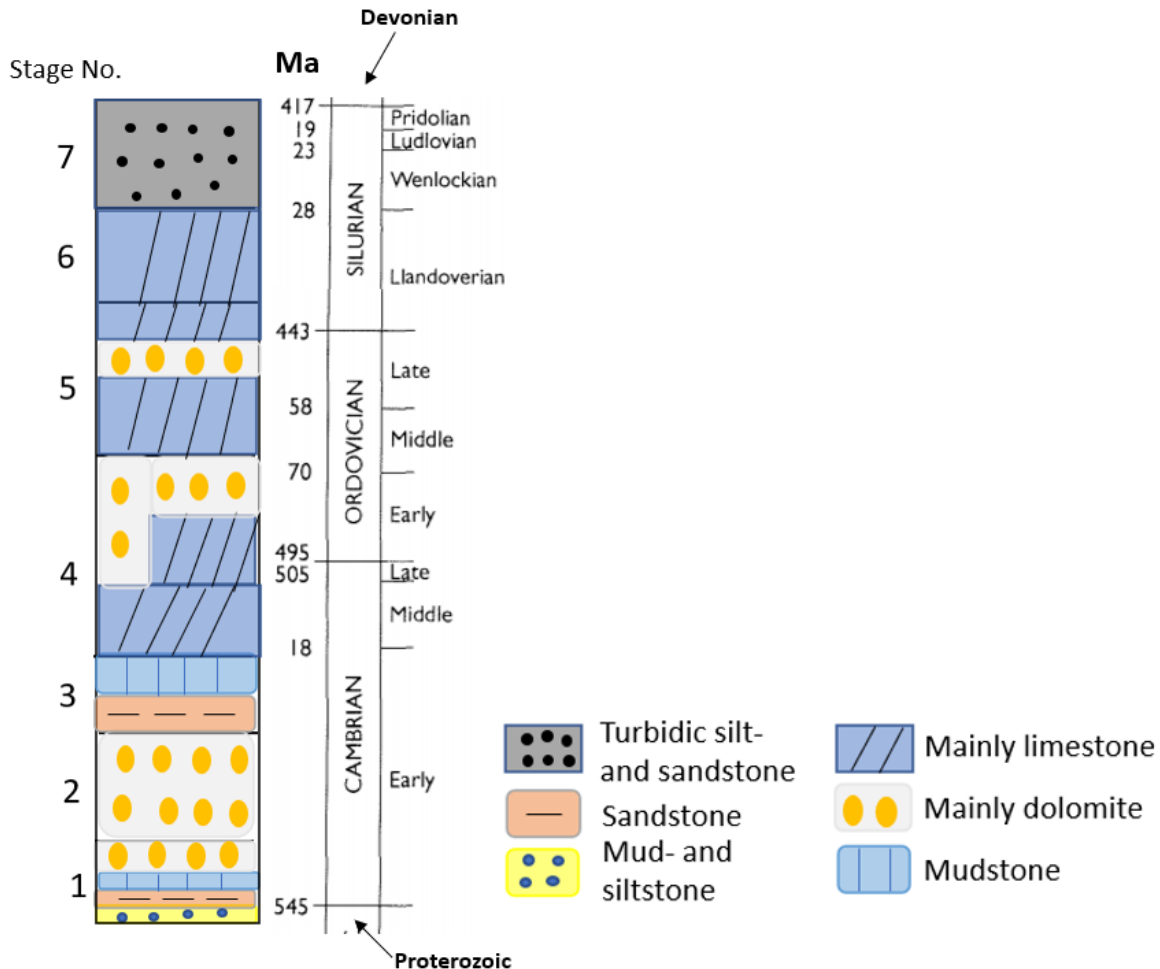


**Figure 13:** General stratigraphic log sequence of the seven stages of the Franklinian Basin, including a time scale showing period and epoch of each of the stages (modified from Henriksen and Higgins, 2000).

#### 4.4 The crystalline basement of the Franklinian Basin

The map from Dawes (2009) was made by basically using nunataks (restricted to the Inland Ice margin within 30 km from nearest land) glacial erratics, drilling and geophysics. The sub-ice bedrock in Rasmussen Land close to the Petermann Fjord and the Sherard Osborn Fjord basically contains porphyries (igneous rocks with large crystals such as gabbro and granite) and redbeds (basically sandstone, siltstone, and shales). The porphyries and redbeds are believed to be Mesoproterozoic. Banded iron formation is possible to find in the redbeds, but they are not that frequent (Dawes, 2009). Another rock type which can be found in Rasmussen Land is dolerite. Some of the types in

Rasmussen Land has been highly affected by hydrothermal alteration, and they are generally red or brown in color. A second major sub-ice rock type are the basins of basalt found around the Kronprins Fredrik Land (*figure 14*). These basalts are tholeiitic flood basalts, and they are believed to be related to the same magmatism event as which formed the dolerites in the Rasmussen Land province which occurred around 1250 Ma ago. A third major sub-ice rock type is the Paleoproterozoic and Archean rocks found in Victoria Province (*figure 14*). These rock types are generally made up of orthogneisses and meta-granitoid rocks with mafic rock units. It is not possible to visually see the difference between the Paleoproterozoic and the Archean rocks in the crystalline basement (*Jepsen & Kalsbeek, 2000*). Instead, isotope age determination is necessary. Zircon U-Pb isotopes were used to get the Archean age which is believed to be around 3000 Ma old (*Hansen et al. 1987*). However, the age determination is not exactly correct because of a strong disturbance which is believed to be caused by an orogenic event (*Jepsen & Kalsbeek, 2000*). The Ellesmere-Inglefield Province contains the Precambrian Shield which is generally made up of greenstone belts and granodioritic rocks like granites and rhyolite (*Shaw et al, 1967*).

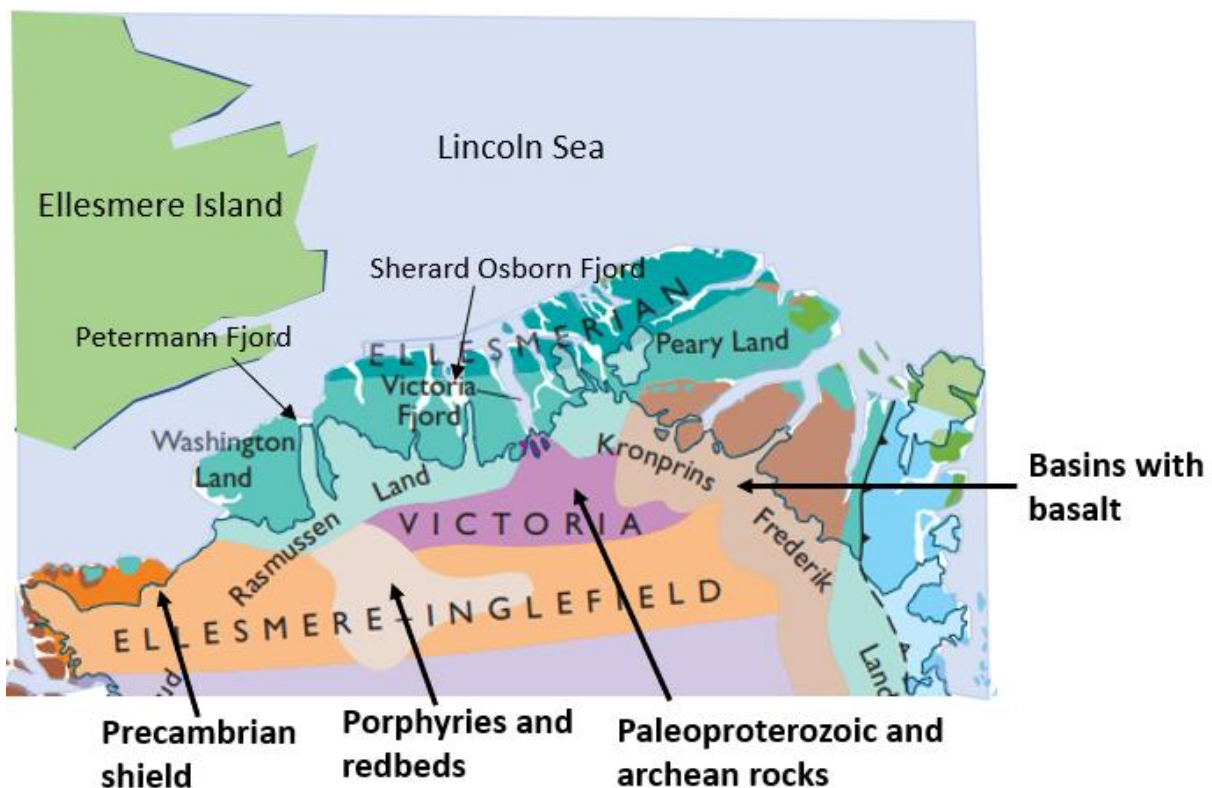


**Figure 14:** The main sub-ice bedrock of the Franklinian Basin. The sub-ice bedrock is in terms of major provinces which are the Rasmussen Land, Victoria, Ellesmere-Inglefield, and Kronprins Fredrik Land. (Figure adapted and modified from Dawes, 2009).

## 5. Methods

In this study, 16 samples from northern Greenland (*Figure 15*) and eight samples from the Lomonosov Ridge off Greenland and the Morris Jessup Rise in the central Arctic Ocean were analyzed. The north Greenland samples were gathered from the core catcher of marine piston and gravity cores. The samples from the Central Arctic Ocean were not taken from the base of the cores because those samples would be hundreds to thousand years old. Instead, they were taken from the first downcore coarse grained interval (between 14-75 cm depth) which was assumed to be from the last glacial cycle. These samples were taken from cores collected on the Arctic Ocean expedition

2016 (AO16), the Lomonosov Ridge off Greenland expeditions in 2007 (LRG07) and 2012 (LRG12). The Ryder samples were gathered in a water depth between 208-867 m and the Central Arctic Ocean samples was gathered in a water depth between 723-1607 m (Table 1).

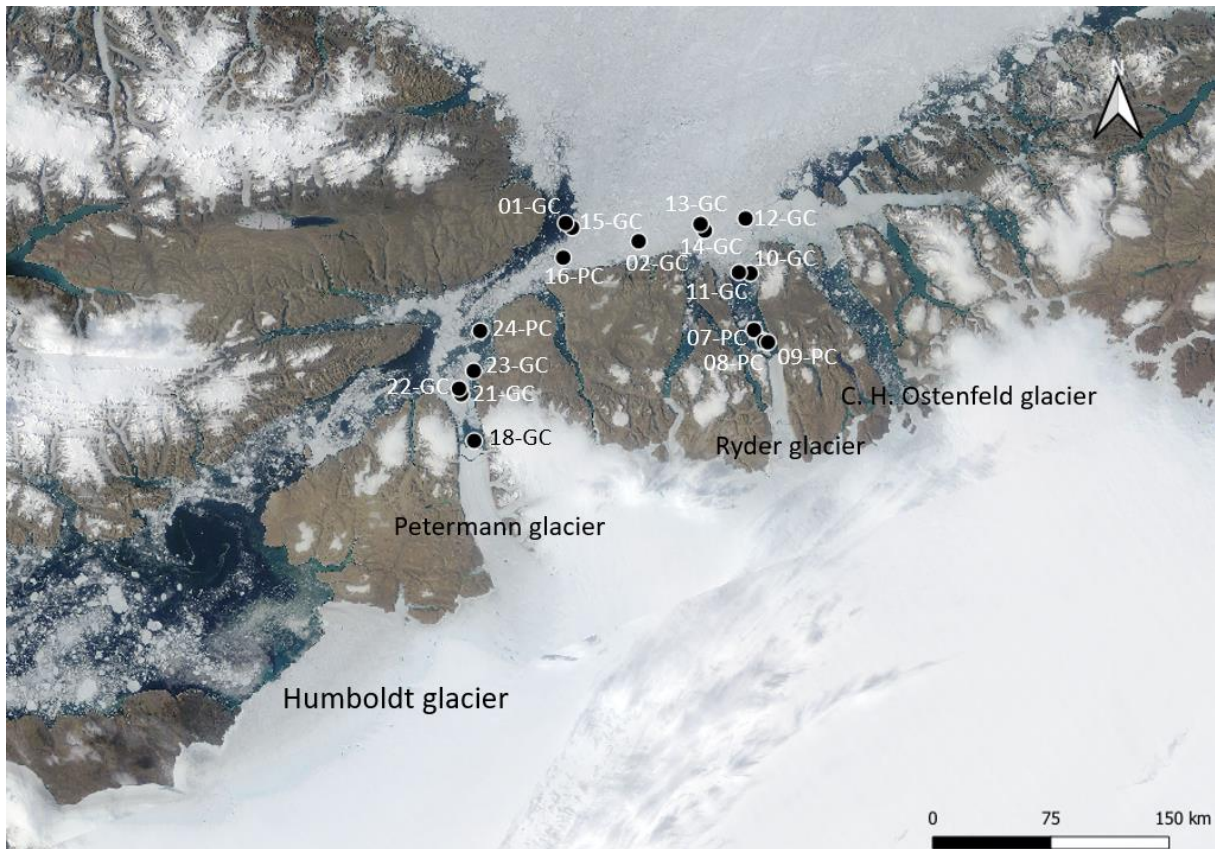


**Figure 15:** Satellite image of the sample locations in the northern Greenland with the four included key glaciers.

### 5.1 Processing northern Greenland samples

Wet samples were put onto a scale to get the weight of the wet samples before being washed through a large diameter 63  $\mu\text{m}$  sieve using tap water. The range of the wet weight was from 21.5 g to 390 g. The >63  $\mu\text{m}$  fraction was transferred into a smaller diameter 63  $\mu\text{m}$  sieve and put into an oven to dry for 24 hours. The dried samples were weighed, and further dry sieved into three different size classes, 63  $\mu\text{m}$  – 1mm, 1-4 mm and >4 mm (Figure 16A). A brush was used to help pass material through the sieves. The amount of material in each size class was weighed and poured into labeled glass vials. A few of the largest clasts >4 mm was stored in plastic bags because some clasts were too large and could not fit into the glass vials (figure 16B).

After sieving, clasts that were >4 mm were counted. The clasts were identified using a hand lens and binocular microscope (figure 16C). The rock fragments were identified as mudstone, sandstone, carbonate rock, granite, gabbro, or amphibolite. Criteria used to identify the rock types included the color, shape, mineral size, and texture. Hydrochloric acid (10% molar) was also used to identify carbonate rock fragments (limestone or dolomite). The total counts, description and identified rock types were recorded. After analyzing the larger clasts, counting and identification of the 1-4 mm size fraction was done. The main characteristics used to identify the rock types were color, shape, and texture. The same rock types were found in the 1–4- mm fraction as they were in the >4 mm fraction. For the 1-4- mm fraction, a binocular microscope was used. As it can be difficult to differentiate

between small clasts of limestone and dolomite, these two rock types were grouped together as “Carbonates”. It was also quite hard to differentiate between siltstone and mudstone, so they were called “mudstone”. No attempt was made to identify clasts in the 63  $\mu\text{m}$  – 1 mm fraction. Five samples could not be used when analyzing the 1-4 mm and >4 mm clasts since these samples lacked rock fragments in this size class. Box plots and pie charts were made from the 1–4 mm clasts.

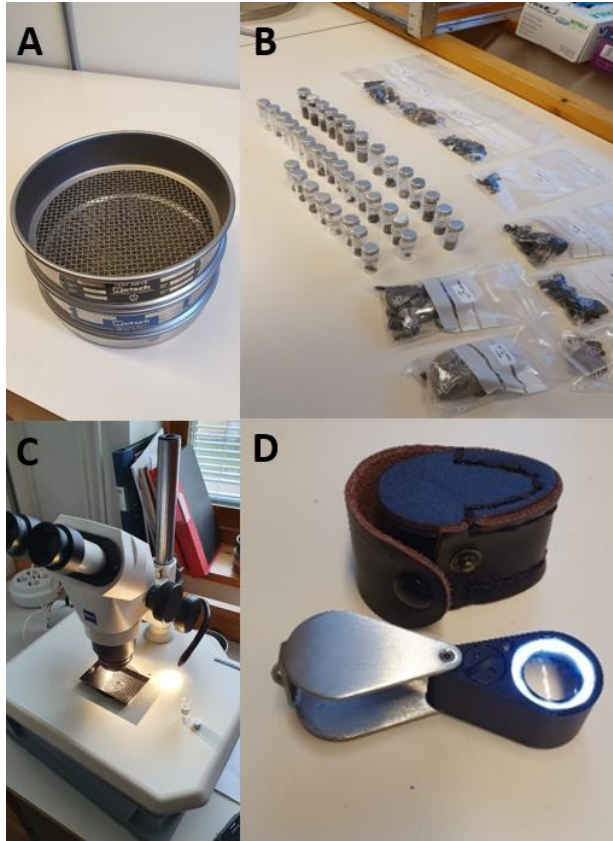


**Figure 16:** The instrument used for the processing of the samples. These are sieves (16A), vials and plastic bags (16B), binocular microscope (16C) and a hand lens (16D).

## 5.2 Processing the Arctic Ocean samples

Wet sieving was not needed for the Central Arctic Ocean samples as the coarse fraction content (>63  $\mu\text{m}$ ) had previously been separated. The samples were dry sieved through a 0.5 mm sieve to separate larger clasts that could be more readily identified. The analysis process was similar to samples from the *Ryder 2019* expedition. The clasts were counted using a binocular microscope and a hand lens (figure 16D). These samples generally contained the same rock types as the *Ryder 2019* samples, but not the exact same amount. The Central Arctic Ocean samples contained a lot of unknown rock types and minerals that were difficult to identify.

| Sample ID            | Lat (N) | Long (E) | Water Depth (m) |
|----------------------|---------|----------|-----------------|
| Ryder19-21-<br>GC-CC | 81.2452 | -62.2735 | 505             |
| Ryder19-24-<br>PC-CC | 81.6215 | -62.296  | 520             |
| Ryder19-22-<br>GC-CC | 81.2715 | -62.4103 | 390             |
| Ryder19-23-<br>GC-CC | 81.3923 | -62.0768 | 343             |
| Ryder19-07-<br>PC-CC | 81.9518 | -51.5878 | 559             |
| Ryder19-09-<br>PC-CC | 81.8908 | -50.9682 | 274             |
| Ryder19-08-<br>PC-CC | 81.8928 | -51.1315 | 238             |
| Ryder19-12-<br>GC-CC | 82.5782 | -52.5277 | 867             |
| Ryder19-14-<br>GC-CC | 82.5087 | -54.4498 | 580             |
| Ryder19-11-<br>GC-CC | 82.2682 | -52.5038 | 208             |
| Ryder19-13-<br>GC-CC | 82.4762 | -54.2215 | 484             |
| Ryder19-15-<br>GC-CC | 82.3502 | -60.1722 | 445             |
| Ryder19-01-<br>GC-CC | 82.334  | -59.8598 | 438             |
| Ryder19-16-<br>PC-CC | 82.1557 | -59.8952 | 415             |
| Ryder19-10-<br>GC-CC | 82.2713 | -52.0165 | 272             |
| Ryder19-02-<br>GC-CC | 82.3467 | -56.9462 | 481             |
| 86.7011              |         |          |                 |
| LRG07-4PC            | 7       | -53.7672 | 811             |
| 85.3198              |         |          |                 |
| LRG07-8PC            | 3       | -14.8575 | 1038            |
| 86.6318              |         |          |                 |
| LRG07-2GC-           | 3       | -54.1512 | 723             |
| 86.6278              |         |          |                 |
| LRG07-3GC            | 3       | -54.959  | 721             |
| 87.7247              |         |          |                 |
| LRG12-3TC            | 2       | -54.4253 | 1607            |
| AO16-5PC             | 89.078  | -130.547 | 1253            |

**Table 1:** Sample number, sample locations (lat and long) and the water depth where the samples were gathered.

### 5.3 Extracting Published Legacy Data

A large spatially distributed data set of 27 samples were published by *Phillips and Grantz (2001)* to illustrate Circum-Arctic clast compositions. However, no tabulated data was in their paper. Instead, they used a small, stacked bar diagrams and a scale bar to present the data of each rock type they found (*Figure 17*). For this project, their data was digitized by matching the scale bar to each stacked diagram for each core location. The samples come from areas like the Lomonosov Ridge and the Eurasian Basin in the eastern Arctic Ocean and Chukchi Sea and the Beaufort Sea around the Amerasian Basin in the western Arctic Ocean and were used to investigate changes in surface circulation patterns of the Beaufort Gyre and Transpolar Drift during glacial periods (*Phillips and Grantz, 2001*).

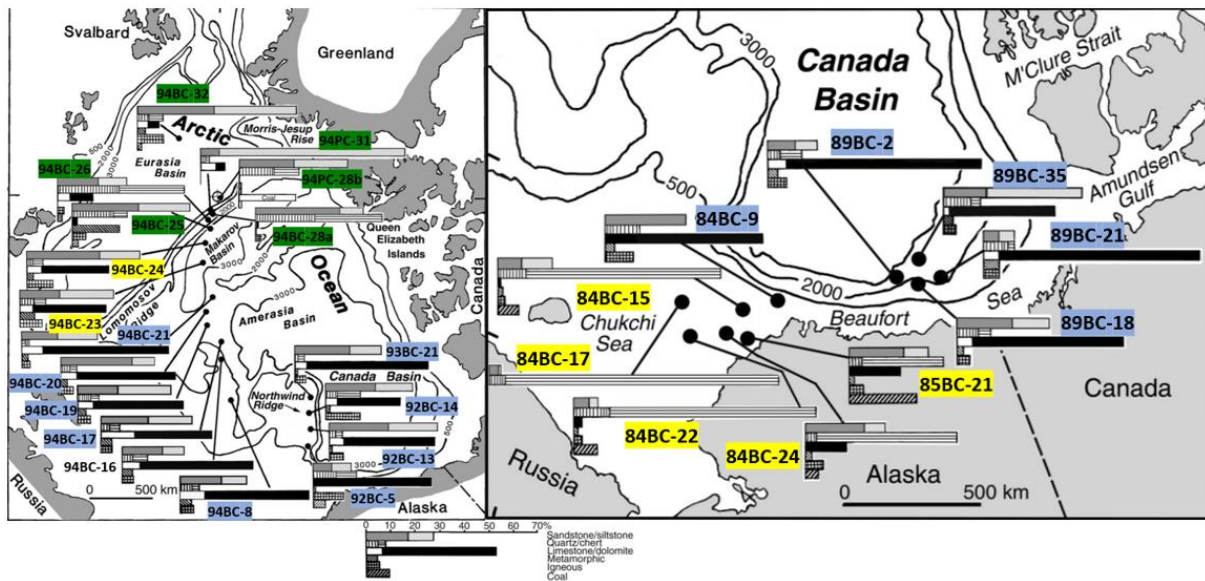


**Figure 17:** Sample locations each area in the Phillips and Grantz study from 2001. Including the stacked bar graph which was digitized into exact number. The Green color is typical Eurasian clast suite, blue color is typical Amerasian clast suite and yellow is not separated into any clast suit.

## 6. Results

The number of >63  $\mu\text{m}$  and 1-4 mm clasts found in the samples was generally not that much. However, some cores had abundant clasts (>2 g) and those are 11-GC with 2.49 g, 23-GC with 11.27 g and 24-PC with 50.87 g (table 2). Sample Ryder19-02-GC and 10-GC had no 1-4 mm clasts. Other samples with insufficient material were 13-GC, 15-GC, and 01-GC. Even though the majority of the clasts from these three samples are between 1-4 mm in size, they had too few clasts (5-6 clasts) to provide meaningful assemblage counts. Samples that were useful for these analyses were samples which had weights of 0.3 g or more and contained at least 10 grains between 1-4 mm in size.

| Sample No.       | 63 $\mu\text{m}$ -1 mm (g) | 1 $\mu\text{m}$ - 4 mm (g) | 63 $\mu\text{m}$ - 4 mm (g) | >63 - 1 mm (%) | 1-4 mm (%) |
|------------------|----------------------------|----------------------------|-----------------------------|----------------|------------|
| Ryder19-21-GC-CC | 1.06                       | 0.75                       | 1.81                        | 58.56          | 41.44      |
| Ryder19-24-PC-CC | 32.06                      | 18.81                      | 50.87                       | 63.02          | 36.98      |
| Ryder19-22-GC-CC | 0.63                       | 0.82                       | 1.45                        | 43.45          | 56.55      |
| Ryder19-23-GC-CC | 3.14                       | 8.13                       | 11.27                       | 27.86          | 72.14      |
| Ryder19-07-PC-CC | 0.28                       | 0.06                       | 0.34                        | 82.35          | 17.65      |
| Ryder19-09-PC-CC | 0.00                       | 0.69                       | 0.69                        | 0.00           | 100.00     |
| Ryder19-08-PC-CC | 0.54                       | 1.20                       | 1.74                        | 31.03          | 68.97      |
| Ryder19-12-GC-CC | 0.40                       | 0.40                       | 0.80                        | 50.00          | 50.00      |
| Ryder19-14-GC-CC | 0.13                       | 0.72                       | 0.85                        | 15.29          | 84.71      |
| Ryder19-11-GC-CC | 1.26                       | 1.23                       | 2.49                        | 50.60          | 49.40      |
| Ryder19-13-GC-CC | 0.01                       | 0.07                       | 0.08                        | 12.50          | 87.50      |
| Ryder19-15-GC-CC | 0.01                       | 0.08                       | 0.09                        | 11.11          | 88.89      |
| Ryder19-01-GC-CC | 0.03                       | 0.11                       | 0.14                        | 21.43          | 78.57      |
| Ryder19-16-PC-CC | 0.65                       | 0.99                       | 1.64                        | 39.63          | 60.37      |
| Ryder19-10-GC-CC | 0.00                       | 0.00                       | 0.00                        | 0.00           | 0.00       |
| Ryder19-02-GC-CC | 0.00                       | 0.00                       | 0.00                        | 0.00           | 0.00       |

**Table 2:** Dry mass (in grams) of the >63  $\mu\text{m}$  and the 1-4 mm size for each sample from northern Greenland. The combined mass for these fractions is also documented. The Arctic Ocean samples were not weighted.

## 6.1 Main rock types

The clasts were separated into 6 rock type categories, and these are mudstone, sandstone, carbonate, granite, gabbro, and amphibolite (*figure 18*).



**Figure 18:** The main rock type categories which are mudstone, sandstone, carbonate, granite, gabbro, and amphibolite.

**Mudstone:** Mudstones are generally brown in color but in some samples, they could also be dark green or black (*figure 18*). Two types of mudstones exist in the samples, one type is flatter, and the other type is more cubic or rectangular. Both types are quite fine grained. Potential clay looking minerals could be spotted in the flatter mudstone but is not seen in the cubic or rectangular ones. The type of minerals was not identified as the rock type is too fine-grained. The flatter mudstone could easily be mistaken for shale instead of mudstone but since it is hard to tell them apart (*figure 18*), they are both called mudstone as a more general term for this type of rock. High amounts of this rock type are found in pretty much every sample from Ryder 2019.

**Sandstone:** The sandstone found in in the samples are generally light brown or pinkish red but light grey sandstones also exists which means that they can be mistaken for carbonates if only color is used as an identification tool. However, using HCL it is possible to tell them apart, as, carbonates will start to corrode compared to the sandstone. The sandstone is also soft compared to many other rock types and extremely fine grained. Only a few samples contain high amount of sandstone.

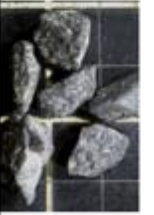
**Carbonates:** The carbonates are generally grey in color, but some carbonate clasts are also lighter or darker brown. The carbonates are quite similar to the grey sandstone and were distinguished

using HCL. Carbonates found in the samples are fine-grained and quite hard. Two types of carbonate rock were most likely found in the samples and those are the dolomite and the limestone. Since these rocks are hard to differentiate from each other in small samples, they were compiled into the same rock type. Large amounts of the carbonate clasts were found in every sample.

**Granite**: The granite in the samples is generally intermediate to mafic and has a red-grey to a little more brown or black color. These granites are generally quite coarse grained and contain larger crystals (porphyry texture). These granites are quartz rich but other minerals that can be seen include feldspar and plagioclase. Medium to low abundance of granites are found in almost every sample except for a few samples that generally contain a large amount of granite.

**Gabbro**: The gabbro found in the samples are coarse grained, mafic, and often black or dark green in color, with some white markings. This rock type also contains large crystals like the granite, which means that it has a porphyry texture. The main dark minerals seen with aid of the hand lens are most likely pyroxene and the white spots likely plagioclase. The abundance of gabbro is generally low in all the samples from northern Greenland.

**Amphibolite**: Amphibolite in the samples is generally dark grey, but a few amphibolite clasts seem to be black or dark green in color, which means that they could be mistaken for mudstone if only color is the identification tool. The amphibolite is generally harder than the mudstone and no clay looking minerals are spotted in the amphibolite, which makes it possible to differentiate them from each other (*Table 3*). This rock type is also quite fine grained which makes it hard to identify the minerals seen in the rocks. The abundance of amphibolite is quite variable in the samples.

| Sample No. | Mudstone   | Sandstone  | Carbonate  | Granite   | Gabbro   | Amphibolite  | Mud vs Amp   |
|------------|--|--|--|---|--|--|--|
| 21-GC      |  |  |  |  |  |  |  |
| 08-PC      |   |   |   |   |   |  |  |
| 12-GC      |   |  |   |   |  |   |   |

**Table 3:** The general appearances of the six main rock types, from a selected group of samples. Rock clasts are from samples 21-GC, 12-GC and 08-GC (one each from the three groups). The mudstone and the amphibolite is also compared to each other in the 12-GC group.

## 6.2 Summary of the counted rock types and abundance of each sample

The total number of clasts (1-4 mm) for each sample had a large range from 0 clasts (sample 10-GC and 02-GC) up to 408 clasts (sample Ryder19-24-PC) (*Table 4*). Other Ryder samples with abundant clasts are sample 23-GC with 220 clasts and 11-GC with 82 clasts. The samples which have less than 10 clasts were not used in the analysis, and they are Ryder19-13-GC, 15-GC, 01-GC (all with 5-6 clasts), 10-GC and 02-GC (with 0 clasts in 1-4 mm size).

The samples from the Arctic Ocean expedition 2016 (AO16) basically have the most clasts of all the Central Arctic Ocean samples (99-103 clasts) while the samples from the Lomonosov Ridge expeditions (LRG07 and LRG12) have between 12-38 clasts in total. The three most abundant rock type for the Arctic Ocean expedition are mudstone (18-27 clasts), sandstone (21-24 clasts), and carbonate (21-29 clasts). The minor rock types are granite (8-11 clasts), gabbro (6-7 clasts), and amphibolite (15 clasts for each Arctic Ocean sample). The three most abundant rock types in the Lomonosov Ridge samples are also the mudstone (3-8 clasts), sandstone (3-9 clasts) and the carbonates (2-9 clasts). The minor rock types from the Lomonosov ridge samples are granite (2-6 clasts), gabbro (0-3 clasts), and amphibolite (3-6 clasts) (*Table 4*).

| Sample No.            | Mudstone | Sandstone | Carbonate rock | Granite | Gabbro | Amphibolite | Total # |
|-----------------------|----------|-----------|----------------|---------|--------|-------------|---------|
| Ryder19-21-GC-CC      | 13       | 5         | 12             | 7       | 3      | 3           | 43      |
| Ryder19-24-PC-CC      | 110      | 53        | 106            | 49      | 41     | 49          | 408     |
| Ryder19-22-GC-CC      | 5        | 2         | 7              | 5       | 1      | 2           | 22      |
| Ryder19-23-GC-CC      | 44       | 20        | 106            | 24      | 11     | 15          | 220     |
| Ryder19-07-PC-CC      | 7        | 2         | 4              | 3       | 2      | 2           | 20      |
| Ryder19-09-PC-CC      | 5        | 1         | 5              | 3       | 2      | 3           | 19      |
| Ryder19-08-PC-CC      | 9        | 8         | 8              | 4       | 8      | 2           | 39      |
| Ryder19-12-GC-CC      | 15       | 1         | 13             | 5       | 1      | 12          | 47      |
| Ryder19-14-GC-CC      | 6        | 6         | 6              | 5       | 3      | 7           | 33      |
| Ryder19-11-GC-CC      | 28       | 7         | 16             | 12      | 5      | 14          | 82      |
| Ryder19-13-GC-CC      | 2        | 0         | 0              | 1       | 0      | 3           | 6       |
| Ryder19-15-GC-CC      | 2        | 1         | 2              | 1       | 0      | 0           | 6       |
| Ryder19-01-GC-CC      | 3        | 0         | 0              | 1       | 0      | 2           | 5       |
| Ryder19-16-PCI-CC     | 10       | 9         | 7              | 4       | 4      | 2           | 36      |
| Ryder19-10-GC-CC      | 0        | 0         | 0              | 0       | 0      | 0           | 0       |
| Ryder19-02-GC-CC      | 0        | 0         | 0              | 0       | 0      | 0           | 0       |
| AO16-5PC-1, 64-66 cm  | 27       | 21        | 21             | 8       | 7      | 15          | 99      |
| AO16-5PC-1, 14-16 cm  | 18       | 24        | 29             | 11      | 6      | 15          | 103     |
| LRG12-T-C3            | 8        | 7         | 8              | 6       | 3      | 6           | 38      |
| LRG07-2-GC 30-31 cm   | 3        | 3         | 2              | 2       | 0      | 2           | 12      |
| LRG07-3-GC, 34-35 cm  | 8        | 9         | 9              | 4       | 3      | 5           | 38      |
| LRG07-4-PC, 74-75 cm  | 4        | 4         | 5              | 3       | 3      | 4           | 23      |
| LRG07-8-PC-, 55-56 cm | 5        | 3         | 7              | 6       | 1      | 3           | 25      |
| LRG07-3-GC, 30-31 cm  | 8        | 5         | 6              | 4       | 2      | 5           | 30      |

**Table 4:** Table of each counted main rock type and the total amount counted for each Ryder sample and Central Arctic Ocean sample.

Samples Ryder19-13-GC and 1-GC show the highest amount of amphibolite, but also had too few clasts to be used when comparing assemblages in the area (figure 19). The same with sample 15-GC which also contained very few clasts. Something that stands out about the mudstone in any sample is that 14-GC is the only sample which has a mudstone abundance below 20% (18% to be exact). The samples with more abundant mudstone than the rest are 07-PC and 11-GC (34% for both) which is not that strange since these samples were taken quite close to each other (figure 15). Two samples containing the fewest sandstone clasts are Ryder19-12-GC (2%) and 09-PC (4-5%). Samples Ryder19-08-PC and 16-PC contain many sandstone grains compared to other samples (around 20-25%). There are no samples containing low amounts of carbonates. The lowest is found in Ryder19 sample 14-GC with an abundance at 18%. However, sample 23-GC is notable in that it has a carbonate abundance of 48%. Samples Ryder19-21-GC, 22-GC and 24-PC are also quite abundant in carbonates (25-31%) indicating that the samples close to the Petermann area are generally quite rich in carbonates. For granite, there is only one sample that stands out. It is sample Ryder19-22-GC which has a granite abundance at 23% and is the only sample with a granite abundance above 20%. Pretty much every sample contains a low amount of gabbro, except sample Ryder19-08-PC with an abundance of 21%. Amphibolite abundance is very scattered ranging from 5% in 08-PC to 26% in 12-GC.

Something that stands out for the Central Arctic Ocean samples is that these samples are generally quite abundant in sandstone (shifting between 12% in the sample with the lowest value to 25% in the sample with the highest sandstone value). The mudstone in the Arctic Ocean area is also generally quite high (17-28% between the highest and the lowest values). The carbonate in these samples is equally abundant in pretty much every Arctic Ocean sample. The minor rock type in these samples is the gabbro (between 4-13%). Something that stands out about the granite is the large number in the sample LRG07-PC-8 (24%). Besides that, granite and the amphibolite in the area are quite similar in abundance (around 10-17 %) for each rock type.

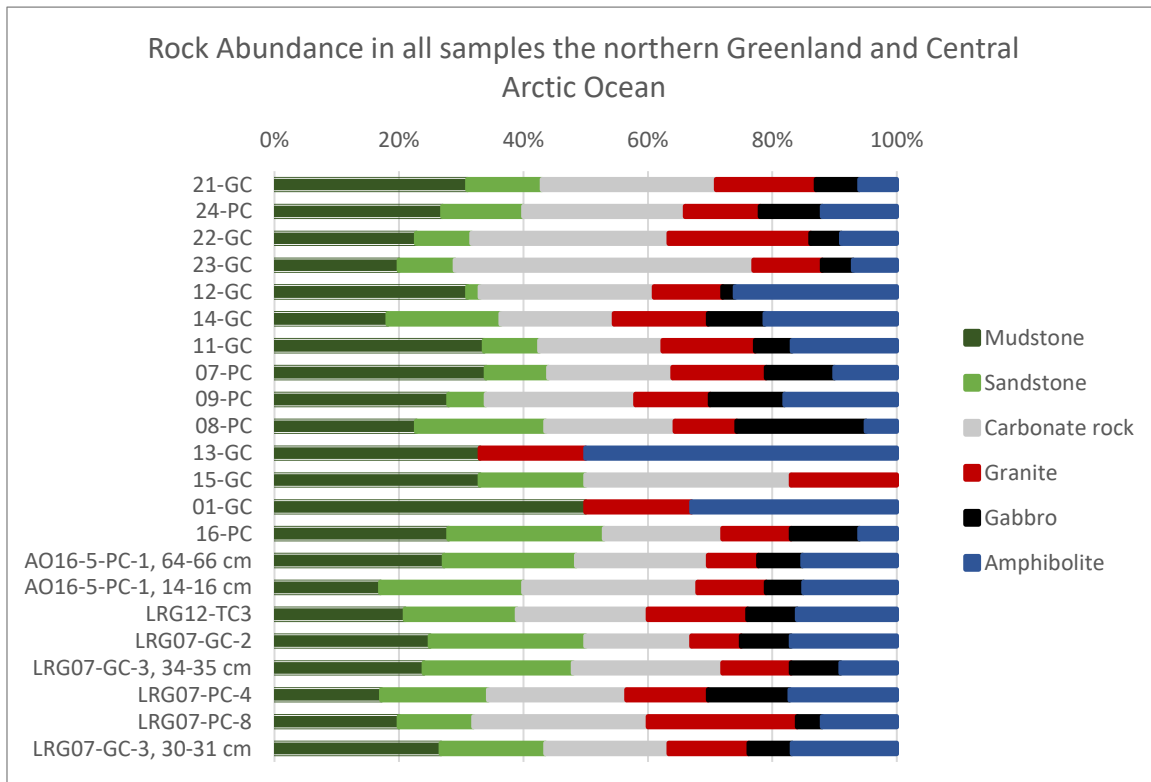


**Figure 19:** Rock abundance in all the samples containing 1-4 mm clasts. Samples with not enough material like Ryder19-13-GC, 15-GC and 01-GC are also shown in the graph. Longer bar means more abundant rock in the sample.

### 6.3 Rock distribution comparison

The clast assemblage was first compared between different regions in northern Greenland (Ryder2019 samples). Firstly, the northern Greenland (NG) samples and the Central Arctic Ocean (CAO) samples were compared, and lastly the northern Greenland samples and the legacy data set of *Phillips and Grantz (2001)* representing the average clast composition across the Amerasian Basin were compared.

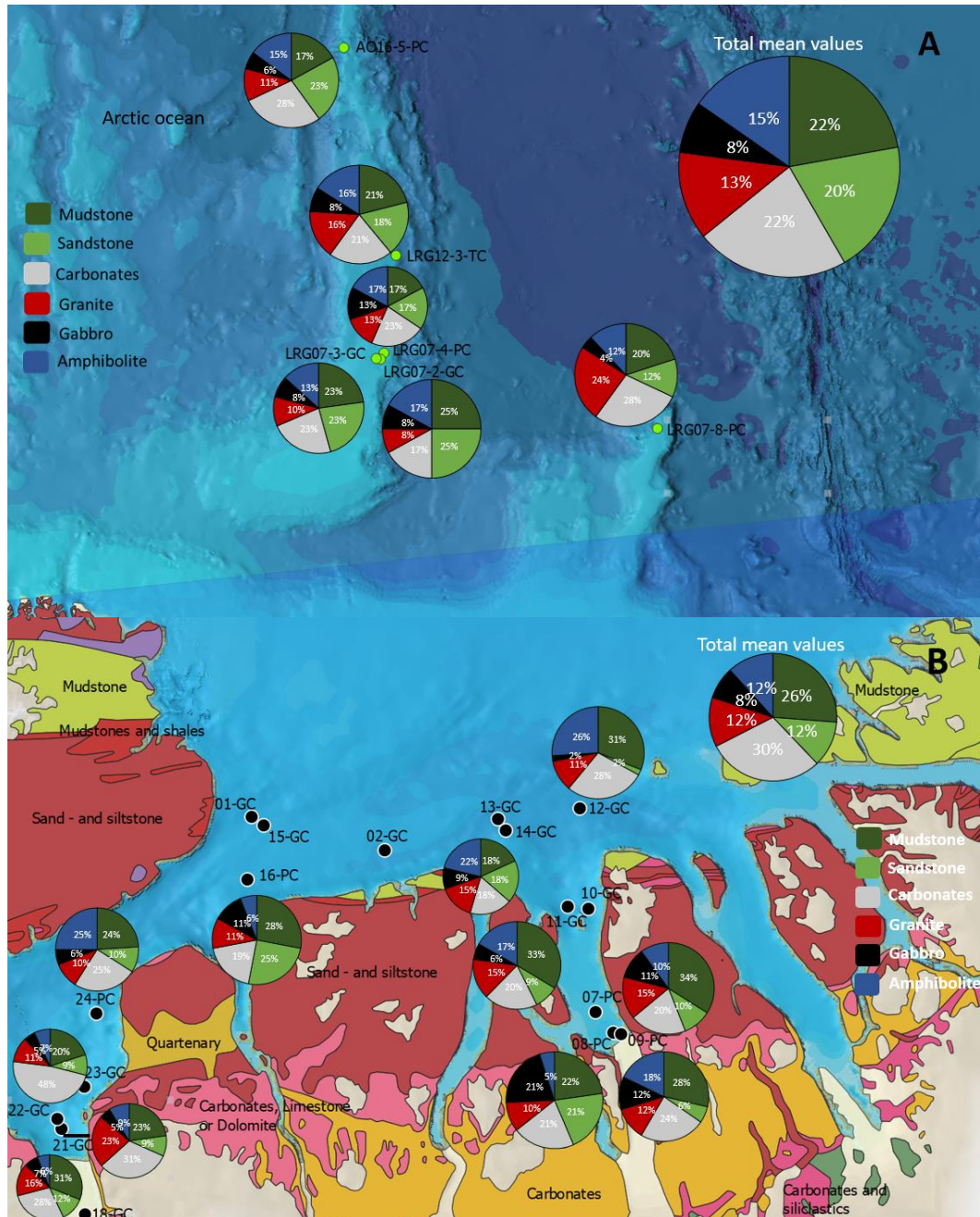


**Figure 20:** The mean rock composition value for each rock type found in the Central Arctic Ocean (20A) and the mean rock composition value for each rock type in the northern Greenland samples (20B). The grain size that was analyzed here was between 1-4 mm.

The carbonate mean abundance in the northern Greenland (NG) samples are as high as 30 % (*figure 20B*) which is a little bit higher than the Central Arctic Ocean (CAO) samples which have a mean abundance of 22 % and a standard deviation at 8.2 (*figure 21*). The mean value of the mudstone in both areas are more similar than the carbonates. The mudstone in NG has a mean value of 26% (and a standard deviation at 5.5), while the mudstone in CAO has a value of 22%. The gabbro in each area has the same mean value. The sandstone abundance in NG is around 12% which is lower than it is in the CAO where it is 20%. The abundance between the granites and the amphibolite's respectively in each area are almost the same. Around 12% granite was found in the NG samples and 13% of granite was found in the CAO samples and 12% mean abundance of amphibolite was found in the NG samples while 15% of the amphibolite was found in the CAO samples (*figure 20A*).

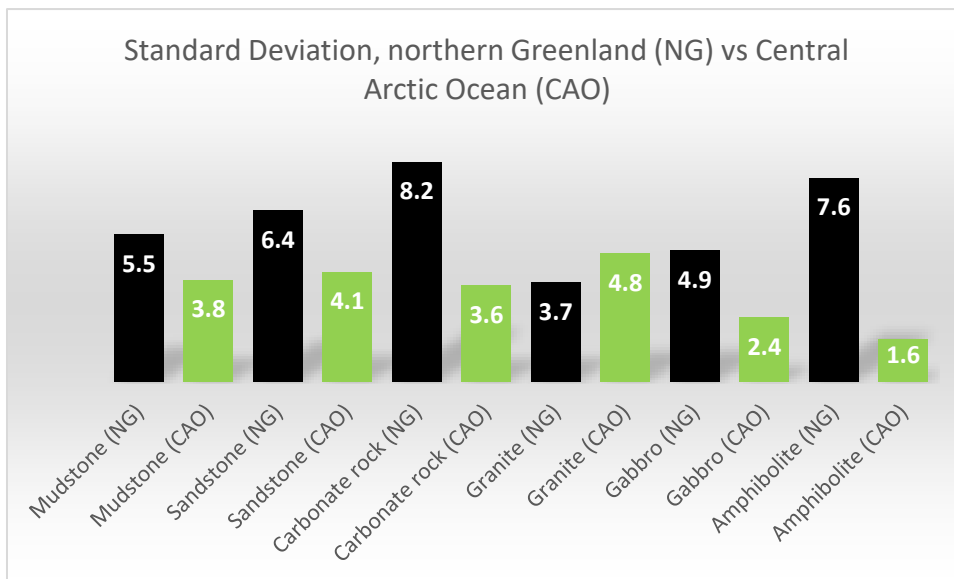


**Figure 21:** Standard deviation measurement of northern Greenland samples compared to the Central Arctic Ocean samples. Higher numbers mean higher differences from the mean value.

A boxplot is basically a standardized way of displaying the distribution of data based on a five-number summary that includes the minimum value, first quartile, median, third quartile and a maximum. Box plots illustrate the distribution of each rock type between the two different areas if the rock composition is grouped or skewed and if the data are symmetrical (*Figure 23*). Grouped rock distribution occurs when the range between the smallest value (minimum value) and the largest value (maximum value) is quite small while skewed rock distribution occurs when the range between the smallest value and the largest value are high. A box plot can show outlier (which a data point that does not fit into the other values) and their values.

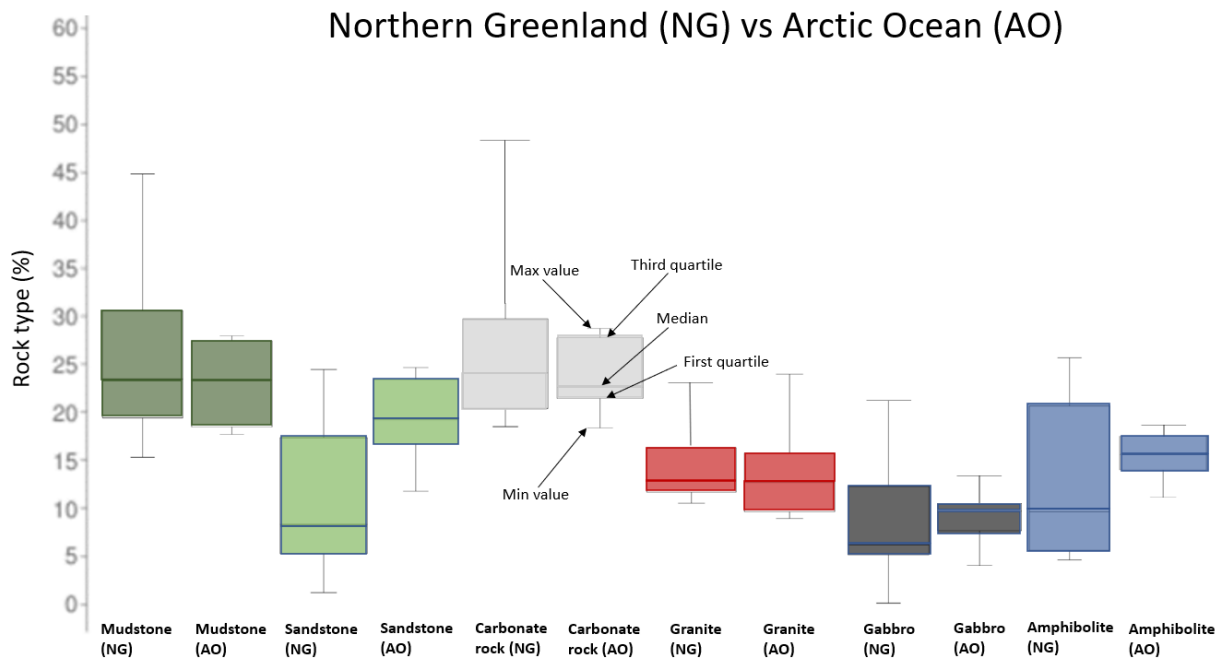


**Figure 22:** The mean value for each rock type in the Ryder samples compared to the Arctic Ocean. Large samples ranges indicate more scattered and small sample ranges indicate more grouped rock distribution. The middle line is the median, the bounds of the colored boxes are the first and third quartile and the top black lines are the maximum value and bottom black line is the minimum value.

It is only one major rock types with similar median values and were the 1<sup>st</sup> and 3<sup>rd</sup> quartiles do not overlap each other in the northern Greenland -and Arctic Ocean samples, and the rock type is mudstone (figure 22). However, the mudstone is more scattered in the northern Greenland samples (15-45%) than in the Arctic Ocean samples (17-26%) which means that a difference in mudstone in these two areas may exist. This also means that the granite is more reflected in the Arctic Ocean samples than in the northern Greenland sample compared to the mudstone. Another rock type which could be reflected in both the Ryder samples and the Arctic Ocean sample is carbonates which has a similar median (22-24%) but they are not equally grouped which means that they can also be different in rock distribution. Sandstone, gabbro, and amphibolite are not similar in the sample assemblages in terms of rock distribution for these areas.

#### 6.4 The legacy data set of Phillips and Grantz (2001)

Phillips and Grantz (2001) separated rock clasts into five major rock type groups. These groups are combined sedimentary mudstone (siltstone) and sandstone, combined igneous rocks (like granite, gabbro, and basalt), metamorphic rock type like amphibolite, carbonate group which generally contained limestone and dolomite, chert, and coal. However, chert and coal are separated into one and the same group here because they are not that important for the comparison since the coal and chert was not found in the northern Greenland samples. The green colored samples are a typical Eurasian clast suite composition, and the blue colored samples are a typical Amerasian clast suite composition (figure 17).

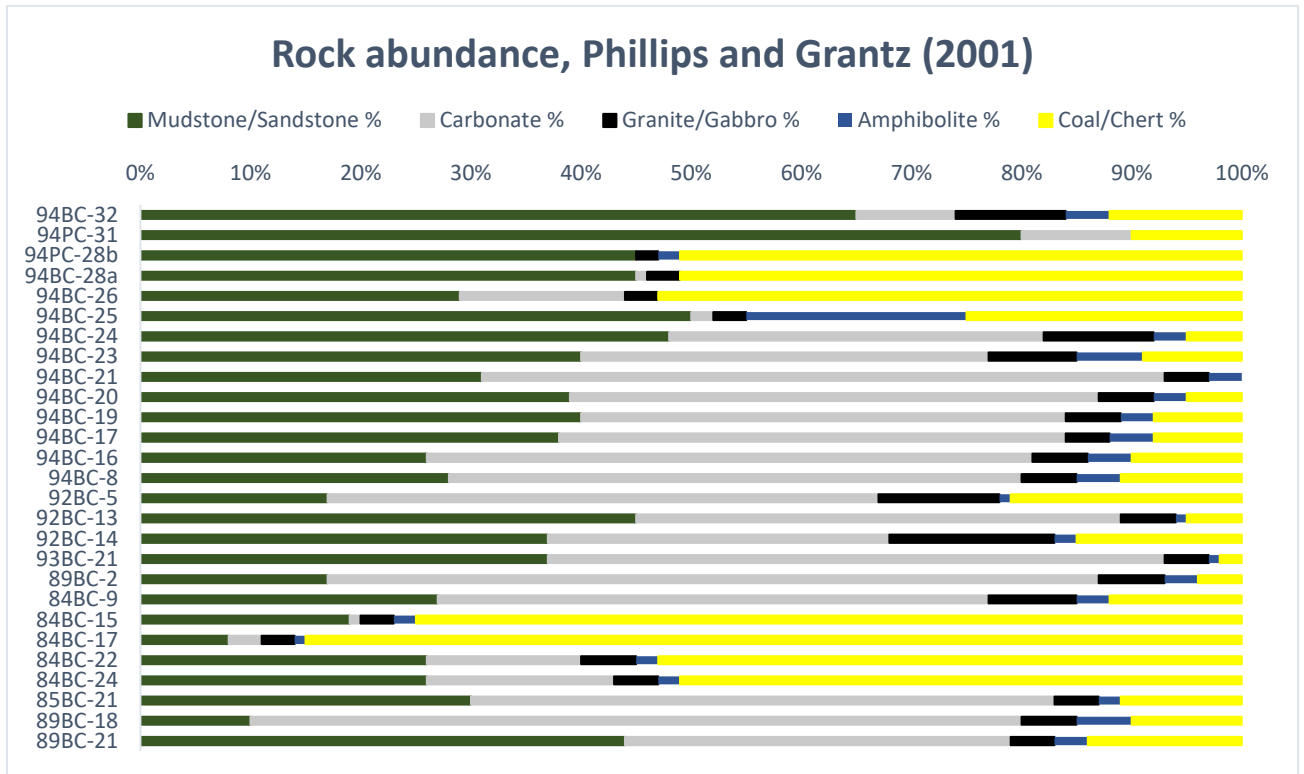


**Figure 23:** This graph shows the rock abundance in the Phillips and Grantz study from 2001, which was conducted around the entire Arctic Ocean.

The samples 94BC-32, 94PC-31, 94PC-28b, 94BC-28a, 94BC-26 and 94BC-25 contain a typical 'Eurasian clasts suite' (as defined by Phillips and Grantz, 2001) and these samples are very abundant in sedimentary rocks like mudstone and sandstone (figure 23). Rarely any carbonates are abundant in this type of clast suite, compared to the 'Amerasian clast suite' which are rich in carbonates. The abundance of carbonate in the Amerasian clast suite can be as high as 70-80%. An example of a typical 'Amerasian clast suite' is sample 94BC-21 which basically contains around 60% carbonates but only around 20% mud- and sandstone which is also something that is typical for the Amerasian clast suite. The sample with the highest abundance of carbonates are 89BC-18 and 89BC-2 which are from the Beaufort Sea area and these two samples have around 70% each. Samples 94BC-32 and 94PC-31 are the most abundant samples in mudstone and sandstone. These samples contain around 65-80% mudstone and sandstone. A lot of samples are also quite even in carbonate and mudstone/sandstone abundance like 94BC-23 which has around 37-40 % of each of these two rock groups. The samples with equal abundance of the two rock groups and samples that contain extraordinarily little of both the rock groups are not separated into Eurasian or Amerasian clasts suites (labeled in yellow in figure 17). The metamorphic (amphibolite) and the igneous rocks are only a minor rock type in pretty much every sample except sample 94BC-25 that contains around 20 % of metamorphic rocks (table 5). A few samples from Phillips and Grantz (2001) only contain a small amount of the four major rock group (mudstone/sandstone, carbonates, igneous and metamorphic). They are instead rich in coal and chert and an example of this is the sample 84BC-17 which has around 85% coal and chert (table 5).

| Sample No.     | Mudstone/<br>Sandstone % | Carbonate % | Granite/Gabbro % | Amphibolite % | Coal/Chert % |
|----------------|--------------------------|-------------|------------------|---------------|--------------|
| 94BC-32        | 65                       | 9           | 10               | 4             | 12           |
| 94PC-31        | 80                       | 10          | 0                | 0             | 10           |
| 94PC-28b       | 45                       | 0           | 2                | 2             | 51           |
| 94BC-28a       | 45                       | 1           | 3                | 0             | 51           |
| 94BC-26        | 29                       | 15          | 3                | 0             | 53           |
| 94BC-25        | 50                       | 2           | 3                | 20            | 25           |
| 94BC-24        | 48                       | 34          | 10               | 3             | 5            |
| 94BC-23        | 40                       | 37          | 8                | 6             | 9            |
| 94BC-21        | 31                       | 62          | 4                | 3             | 0            |
| 94BC-20        | 39                       | 48          | 5                | 3             | 5            |
| 94BC-19        | 40                       | 44          | 5                | 3             | 8            |
| 94BC-17        | 38                       | 46          | 4                | 4             | 8            |
| 94BC-16        | 26                       | 55          | 5                | 4             | 10           |
| 94BC-8         | 28                       | 52          | 5                | 4             | 11           |
| 92BC-5         | 17                       | 50          | 11               | 1             | 21           |
| 92BC-13        | 45                       | 44          | 5                | 1             | 5            |
| 92BC-14        | 37                       | 31          | 15               | 2             | 15           |
| 93BC-21        | 37                       | 56          | 4                | 1             | 2            |
| 89BC-2         | 17                       | 70          | 6                | 3             | 4            |
| 84BC-9         | 27                       | 50          | 8                | 3             | 12           |
| 84BC-15        | 19                       | 1           | 3                | 2             | 75           |
| 84BC-17        | 8                        | 3           | 3                | 1             | 85           |
| 84BC-22        | 26                       | 14          | 5                | 2             | 53           |
| 84BC-24        | 26                       | 17          | 4                | 2             | 51           |
| 85BC-21        | 30                       | 53          | 4                | 2             | 11           |
| 89BC-18        | 10                       | 70          | 5                | 5             | 10           |
| 89BC-21        | 44                       | 35          | 4                | 3             | 14           |
| <b>Average</b> | 35.07                    | 33.67       | 5.33             | 3.11          | 22.81        |

**Table 5:** Rock type distribution from Phillips and Grantz (2001). Core locations measured in degrees, minutes, and seconds are also included.

## 6.5 Statistical testing of clast compositions

A one-way Analysis of variance (ANOVA) test can be used to determine if there is a significant difference between the means of three or more groups. The two important values that are calculated when doing an ANOVA test is the F-ratio value and the F-critical value. The “null hypothesis” in the ANOVA is that no significant differences in means between groups exist. If the calculated F-ratio value is higher than the F-critical value it means that the null hypothesis can be rejected. Another important value are the P-value and the significance level, which was set to 0.05 (95% significance level). If the P-value is lower than the significance level, the “null hypothesis” can also be rejected. Samples from Ryder 2019 expedition were firstly divided into three groups based on qualitative differences. The groups are Petermann Fjord, Lincoln Sea, and the Sherard Osborn Fjord. The Petermann group contains sample Ryder19-22-GC, 21-GC, 23-GC, and 24-PC and defines the ‘Petermann fjord’ assemblage. Lincoln Sea group contains samples Ryder19-13-GC, 14-GC, 12-GC, and defines the ‘Lincoln Sea’ assemblage. Sherard Osborn group contains samples 07-GC, 08-GC, and 09-GC and defines the ‘Sherard Osborn Fjord’ assemblage. An ANOVA test comparison was made between the Petermann Fjord, the Lincoln Sea, and the Sherard Osborn Fjord for each rock type to see if there actually are any significant differences between these areas.

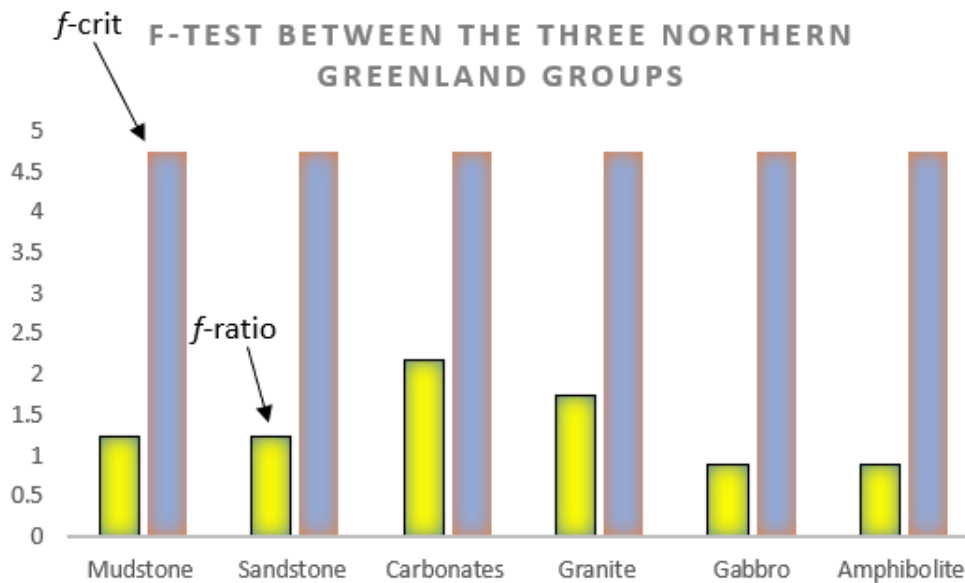


**Figure 24:** Anova test (or F-test) between the three different qualitative groups in the northern Greenland area. Important factors are the  $f$ -crit and the  $f$ -ratio.

The ANOVA test between the three regions of northern Greenland indicates that the F-ratio of any of the major rock types is not higher than the F-critical ratio (at 4.7) (Figure 24). This means that the “null hypothesis” of each rock type cannot be rejected. Since the p value for all the rock types between the groups are higher than 0.05, it also means that the “null hypothesis” cannot be rejected implying that no significant differences between the rock types are found in those three compared groups. The F-ratio value can also give an idea on how similar the compared groups are. Lower F-ratio value for the rock types indicates that they are more similar than if the F-ratio value for each rock type was high. This basically means that the two most similar rock types with the most similar sample means are the gabbro and the amphibolite since they got the lowest F-ratio value (below 1). The largest difference between the areas is for carbonate, since this rock type has the highest F-ratio value (figure 24 and table 6).

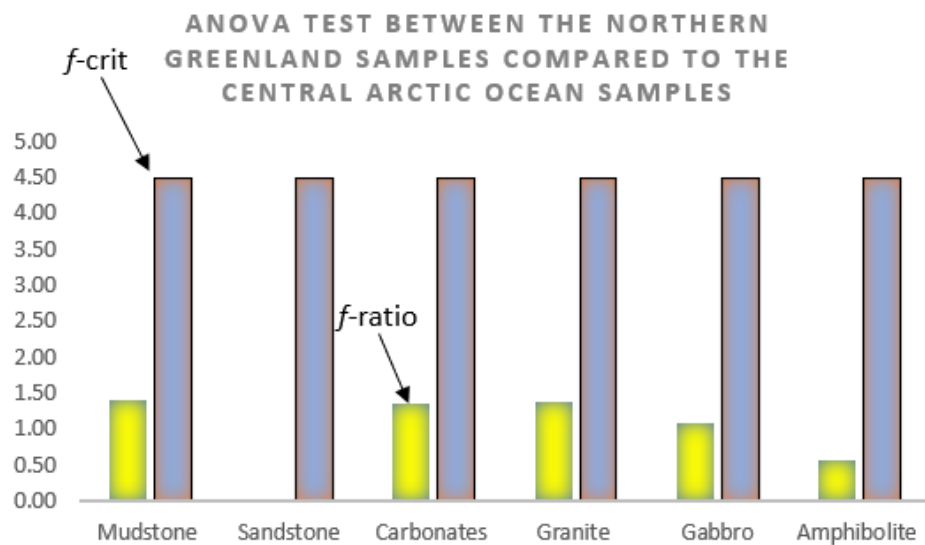


**Figure 25:** ANOVA test (or F-test) between the Ryder samples in the northern Greenland area and the Central Arctic Ocean area. Important factors are the  $f$ -crit and the  $f$ -ratio.

Since there are no significant differences in the clast compositions of the Ryder 2019 samples, they were all grouped together and compared to the Central Arctic Ocean samples. This shows that the F-ratio value in all the rock types is quite low (not higher than 1.5). Since the F-crit ratio is around 4.5 (figure 25), it means that the “null hypothesis” again cannot be rejected, which is supported by the P-value for all the rock types being higher than 0.05 (Table 7). Therefore, statistically, there are no significant differences between the clast abundances between northern Greenland and the Central Arctic Ocean samples in this study. Since the sandstone almost got 0 in F-ratio value, the sandstone mean value between the northern Greenland samples and the Central Arctic Ocean samples are quite similar. The rock types with the highest F-ratio are mudstone, carbonate and the granite implying that they have the largest difference between regions.

| Rock types  | M (PF) | V (PF) | M (LS) | V (LS) | M (SOF) | V (SOF) | SS (BG) | SS (WG) | Df (BG) | Df (WG) | MS (BG) | MS (WG) | F    | P-value | F-crit |
|-------------|--------|--------|--------|--------|---------|---------|---------|---------|---------|---------|---------|---------|------|---------|--------|
| Mudstone    | 43     | 2289   | 16     | 122    | 7       | 3.2     | 2520    | 7118    | 2       | 7       | 1260    | 1016    | 1.24 | 0.35    | 4.7    |
| Sandstone   | 20     | 548    | 4.75   | 11.4   | 3.73    | 15.1    | 599     | 1698    | 2       | 7       | 299     | 242     | 1.24 | 0.35    | 4.7    |
| Carbonate   | 58     | 3103   | 12     | 28.7   | 5.65    | 5       | 5822    | 9378    | 2       | 7       | 2911    | 1339    | 2.17 | 0.18    | 4.7    |
| Granite     | 21     | 417    | 7.5    | 17.5   | 3.2     | 0.38    | 639     | 1287    | 2       | 7       | 319     | 183     | 1.74 | 0.24    | 4.7    |
| Gabbro      | 14     | 339    | 3      | 3.96   | 4.14    | 12.3    | 264     | 1052    | 2       | 7       | 132     | 150     | 0.88 | 0.46    | 4.7    |
| Amphibolite | 17     | 488    | 11     | 13.3   | 2.3     | 0.4     | 382     | 1492    | 2       | 7       | 191     | 213     | 0.9  | 0.45    | 4.7    |

**Table 6:** Calculated values during the ANOVA test between the three qualitative groups. Significant level was set to 0.05 for all the rock types. PF=Peterman Fjord; LS=Lincoln Sea; SOF=Sherard Osborn Fjord; BG=Between Groups; WG=Within Groups. Other factors calculated during the ANOVA test is the mean (M), the variance (V), sum of square (SS), degree of freedom (Df), mean square (MS).

| Rock types  | M (NG) | V (NG) | M (AO) | V (AO) | SS (BG) | SS (WG) | Df (BG) | Df (WG) | MS (BG) | MS (WG) | F     | P-value | F-crit |
|-------------|--------|--------|--------|--------|---------|---------|---------|---------|---------|---------|-------|---------|--------|
| Mudstone    | 24.2   | 1063   | 10.1   | 67.8   | 880     | 10048   | 1       | 16      | 880     | 628     | 1.4   | 0.25    | 4.49   |
| Sandstone   | 10.5   | 254.5  | 9.5    | 69     | 4.44    | 2774    | 1       | 16      | 4.44    | 173.4   | 0.025 | 0.88    | 4.49   |
| Carbonate   | 28.3   | 1691   | 10.9   | 85     | 1349.5  | 15816   | 1       | 16      | 1349.5  | 988.5   | 1.37  | 0.26    | 4.49   |
| Granite     | 11.7   | 212    | 5.5    | 8.58   | 170.8   | 1970    | 1       | 16      | 170.8   | 123.1   | 1.39  | 0.26    | 4.49   |
| Gabbro      | 7.7    | 147.3  | 3.1    | 5.55   | 93      | 1364    | 1       | 16      | 93      | 85      | 1.09  | 0.31    | 4.49   |
| Amphibolite | 10.9   | 206    | 6.9    | 26.7   | 72      | 2043    | 1       | 16      | 72      | 127.75  | 0.56  | 0.46    | 4.49   |

**Table 7:** Calculated values during the ANOVA test between the northern Greenland samples and the Central Arctic Ocean. Significant level was set to 0.05. NG=Northern Greenland; AO=Arctic Ocean; BG=Between Groups; WG= Within Groups.

A final comparison was made between the Ryder 2019 samples and the typical ‘Amerasian clast suite’ of each rock type. A T-test is usually done to compare how similar or different two independent groups are. The factors measured with a T-test are the T-value, the P-value, and the T-critical value. A significance level was set to 0.05 for this test. Just like the Anova test, the “null hypothesis” is that there are no differences between the means. If the T-value is higher than the T-critical value and the P-value is lower than the significance level, it means that the “null hypothesis” is rejected. This seems to be the case for every rock group (Table 8). An example of this is the igneous rocks of granite and gabbro, with a T-value at 9.23 but a T-critical value of only 2.09. This means that there are significant differences between the granite and gabbro between the groups. The same results are also seen because the P-value for each rock type is lower than the significant level (0.05) which means that the “null hypothesis” can be rejected which indicates that there are differences between the northern Greenland samples and the ‘Amerasian clast suite’ from Phillip and Grantz (2001).

| T-test  | Mudstone/<br>Sandstone | Carbonate            | Granite/Gabbro       | Amphibolite |
|---------|------------------------|----------------------|----------------------|-------------|
| T-value | 2.91                   | -7.65                | 9.23                 | 4.33        |
| P-value | 0.008                  | $2.33 \cdot 10^{-7}$ | $1.2 \cdot 10^{-10}$ | 0.0003      |
| T-crit  | 2.09                   | 2.09                 | 2.09                 | 2.09        |

**Table 8:** Calculated T-value and P-value between each northern Greenland samples and a typical Amerasian clast suit from Phillip and Grantz (2001). Significance level is again set to 0.05.

## 7. Discussion

The first aim of the study was to determine the composition and variability of ice rafted clasts along the northern Greenland coast, and evaluate regional variations in clast assemblages. The second aim was to assess whether these clasts can be used to constrain and reconstruct deglacial ice flow patterns of northern Greenland and the Arctic. The third aim was to evaluate whether the clast composition from this region of the Arctic is unique and can be used to identify the provenance of ice rafted material in distal sediment records from the Arctic. Example of distant sediment record could be from other parts of the Arctic Ocean like the Beaufort -and the Chukchi Sea which lie to the far west.

### 7.1 Clast composition and links to past ice flow in northern Greenland

The carbonate is a commonly used indicator of for IRD provenance across the Arctic, as its occurrence is widely assumed to be restricted to the Canadian Arctic and Mackenzie River corridor (Fagel *et al.*, 2014). Results from this study also show that the platform carbonates of the Franklinian Basin also deliver large amounts of limestone/dolomite IRD to the Lincoln Sea (generally between 20-30%).

Carbonate clasts are most abundant in the Petermann Fjord region of the study area. This likely reflects the fact that carbonate sediments of the Franklinian Basin are outcropping directly at the coastline in this region. According to Jakobsson *et al* (2018), the mapped glacial landforms in front of the Petermann fjord indicate that the glacial ice exiting Petermann Fjord traveled northeast, joining the Nares Strait ice stream flowing towards the Lincoln Sea. Here it would have joined the massive Greenland-Ellesmere Ice Shelf, which has its borders in the northern coast of Greenland and Ellesmere Island (figure 26). The high carbonate clast concentration of the Ryder cores reflects this northward ice flow pattern, and contrasts with the more carbonate poor composition of sediments in Kane Basin and Baffin Bay (Caron *et al*, 2020)., These sediments are instead dominated by igneous and metamorphic rocks like Archean orthogneisses, which are believed to be a part of the Precambrian shield. A large part of the Precambrian shield forms the sub-ice bedrock of Greenland (Dawes, 2009).

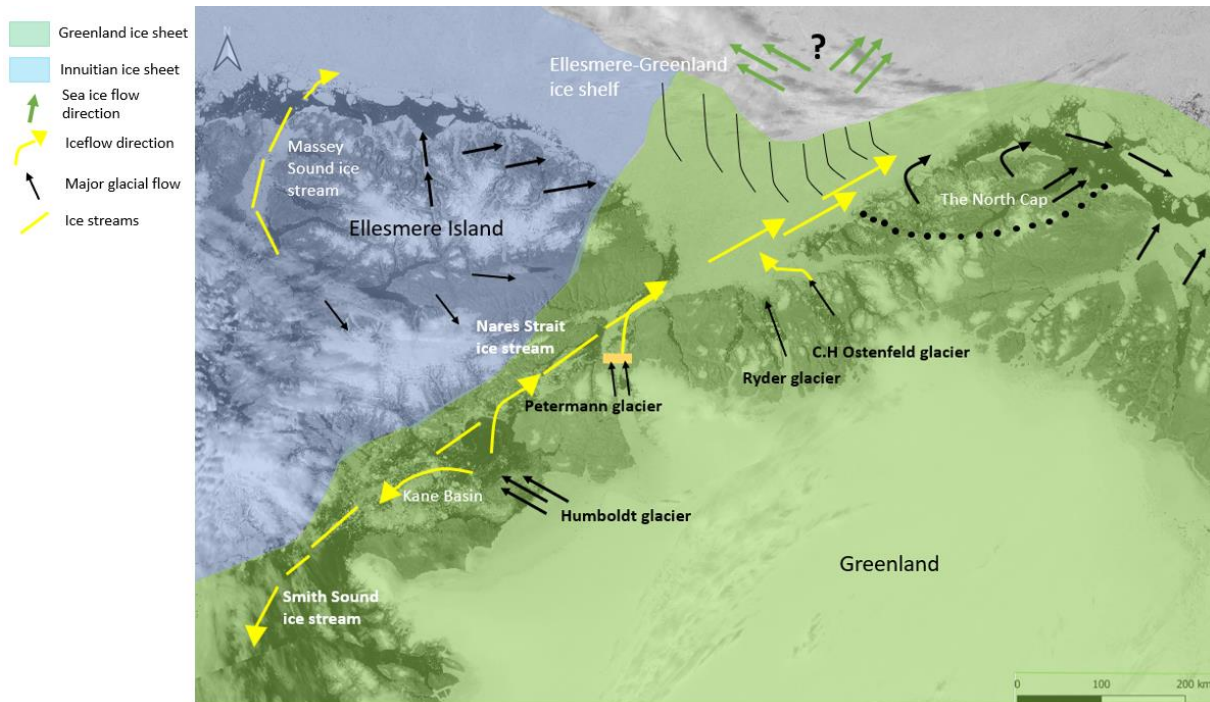


**Figure 26:** Overview map of the ice movement on and around the Greenland ice sheet and Innuitian ice sheet with major glacial flow (black arrows), ice streams (yellow lines) and a potential sea ice flow direction (green arrows) which is marked with a “question mark” since we do not really know the flow direction of the sea ice.

There are a lot of glacial paleo- glaciers and ice streams that operated along the coast of the northern Greenland. One major glacial ice stream is coming from the Humboldt Glacier in eastern Kane Basin. According to England (2006) this ice stream had two different ice flow patterns. Part of it flowed south where it joined the Smith Sound Ice Stream to the southwest and the other part flowed north to join the Nares Strait Ice Stream traveling towards the Petermann Fjord and Lincoln Sea. Another major ice stream came from Petermann Fjord, where the Petermann ice tongue extended into Nares Strait before the ice retreated during deglaciation (Rignot et al, 2001). Since glacial landforms were found pointing towards northeast of Greenland, it is suggested that the Petermann glacial ice traveled east (Jakobsson et al, 2018).

Another indicator of an east-going glacial ice flow from the Petermann area, is detected because samples from the Lincoln Sea area that contain a large abundance of carbonates (20-25%) which most likely has to come from the Petermann direction since that is the only area where carbonates are outcropping directly at the coastline. However, a fast-going ice stream is also moving from the Ryder Glacier through the Sherard Osborn Fjord. At the south end of the Sherard Osborn Fjord, cliffs of carbonate can be found which could indicate that another source of the carbonate clasts are from the Ryder Glacier.

A fourth glacier that flowed into the Lincoln Sea came from Victoria Fjord (C.H Ostenfeld Glacier) (Figure 26) (Rignot et al, 2001). Since the Lincoln Sea samples are quite abundant in amphibolite compared to the samples in the Petermann area and the Sherard Osborn Fjord area, it is likely that source of these clasts is from the south end of the Victoria Fjord. If they are from this region, the amphibolite’s has most likely been carried out by the C.H Ostenfeld Glacier. This is the only coastal area on northern Greenland where amphibolite outcrops exist. Somehow, the east flowing Nares Ice Stream merged with Ryder Glacier and the westerly flowing C.H. Ostenfeld Glacier before being deflected or incorporated into the Ellesmere-Greenland Ice Shelf. A lack of bathymetric data makes it difficult to resolve the ice flow routes in the region.

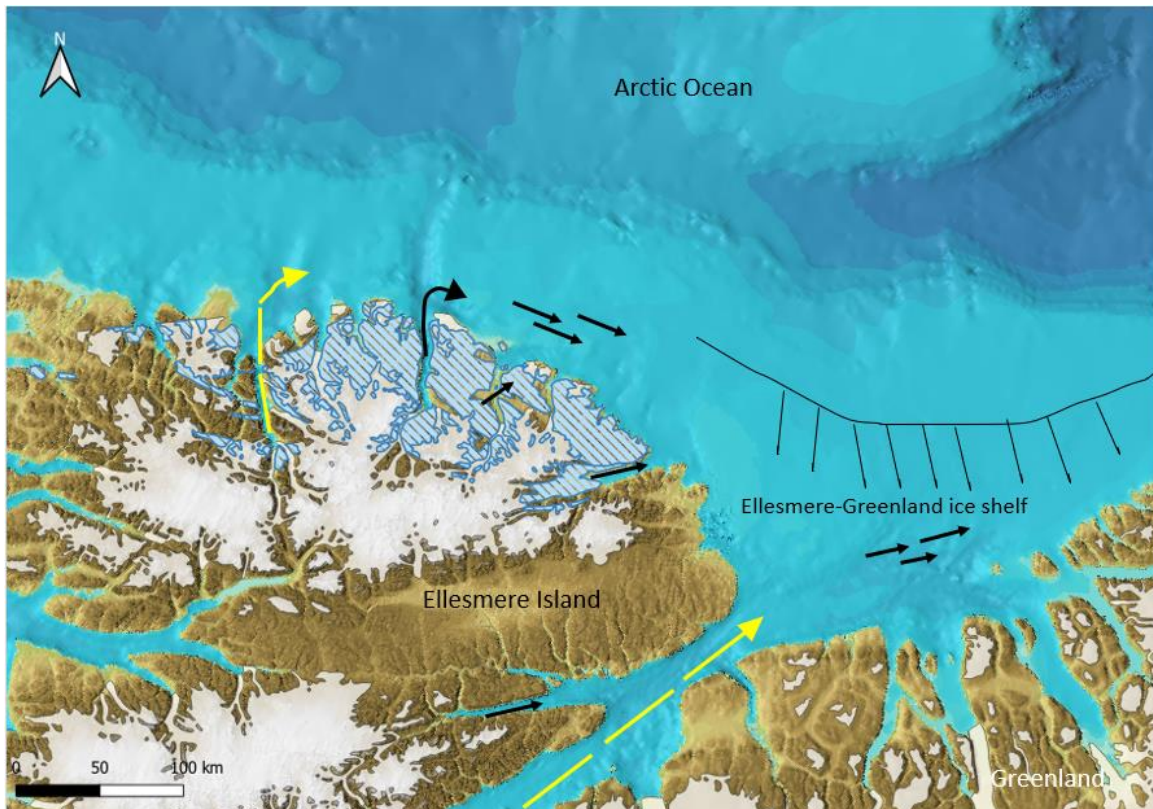


**Figure 27:** Map of Ellesmere Island with the Pearya land marked (which contains amphibolite) and east going ice flow which indicates that amphibolite clasts could have traveled east by ice and then merged with the Ellesmere-Greenland Ice Shelf and then deposited in the northern Greenland area.

The Lincoln Sea sediments thus have a mixed IRD clast signal, which would explain the lower carbonate rate compared to Petermann Glacier and the higher amphibolite abundance that may have come from C.H. Osterfeld Glacier. However, it remains possible that the Ellesmere Island ice merged to the east with the Ellesmere-Greenland Ice Shelf and delivered amphibolite to the Lincoln Sea. The Pearya region found in northern Ellesmere Island is quite rich in amphibolite's and other metamorphic rocks (Trettin, 2011). The amphibolite could have simply been transported by fast flowing ice streams occurring in and around Ellesmere Island (figure 27) since these ice streams are also travelling to the east of the Island (Dawes, 1986). Glaciers from Ellesmere Island could also have delivered argillaceous basin deposits (clay minerals and mudstone) coming from the Sverdrup Basin which could have been carried out to the Arctic Ocean by the Massey Sound Ice Stream. However, XRF measurements are most likely needed to be used for the northern Greenland samples to be able to identify potential clay minerals.

Through analysis and ANOVA testing, it is clear that there are not significant differences between the northern Greenland samples and the Central Arctic Ocean samples. This basically means that the same rock types are reflected in both clast assemblages. One interpretation of the data is that the Lincoln Sea ice extended out across the Lomonosov Ridge and Morris Jessup Rise. It is however not clear how this was done. There is most likely two possible explanations for this. The east flowing Ellesmere-Greenland Ice Shelf was much wider than drawn in published reconstructions (Jakobsson et al, 2014) or that after the east flowing shelf ice broke up around 10 ka years ago (Larsen et al, 2010), more icebergs from northern Greenland were able to travel further into the Central Arctic and deposit IRD. Testing this hypothesis would require dating the analyzed samples using  $^{14}\text{C}$  on foraminifera or other carbonate shelled macrofossils. Something that is not that easy to understand is how the icebergs moved to the Lomonosov Ridge. Iceberg movements are generally dictated by

sea ice flow. However, no one really knows for sure how the sea ice circulation in the Arctic Ocean looked during the last deglaciation. Using clast provenance studies, *Bischof and Darby (1997)* suggested that the sea ice was at first drifting west in front of Ellesmere Island but then changed direction towards east and travelled across the Lomonosov Ridge and out towards the Fram Strait (*figure 28*). If *Bischof and Darby's (1997)* theory is correct about the sea ice movement of Arctic Ocean, it could also indicate that the icebergs traveled from the Lincoln Sea in this modified Beaufort Gyre system before depositing a similar IRD clast composition in the Lomonosov Ridge and the Morris Jessup Rise (*Figure 28*). However, this hypothesis is not readily compatible with evidence for the large east flowing Ellesmere-Greenland Ice Shelf. However, there are three examples which could make this hypothesis true, A) the similarities in IRD was because it was deposited before or after the Ellesmere-Greenland Ice Shelf was in place, B) the IRD similarities indicate a more extensive ice shelf, the icebergs breaking off the northern margin of the ice shelf, or sudden IRD inputs when the ice shelf broke up or C) the similarity in IRD clast composition is a coincidence – and that the central Arctic samples have a mixed clast composition of the Amerasian and Eurasian suites.

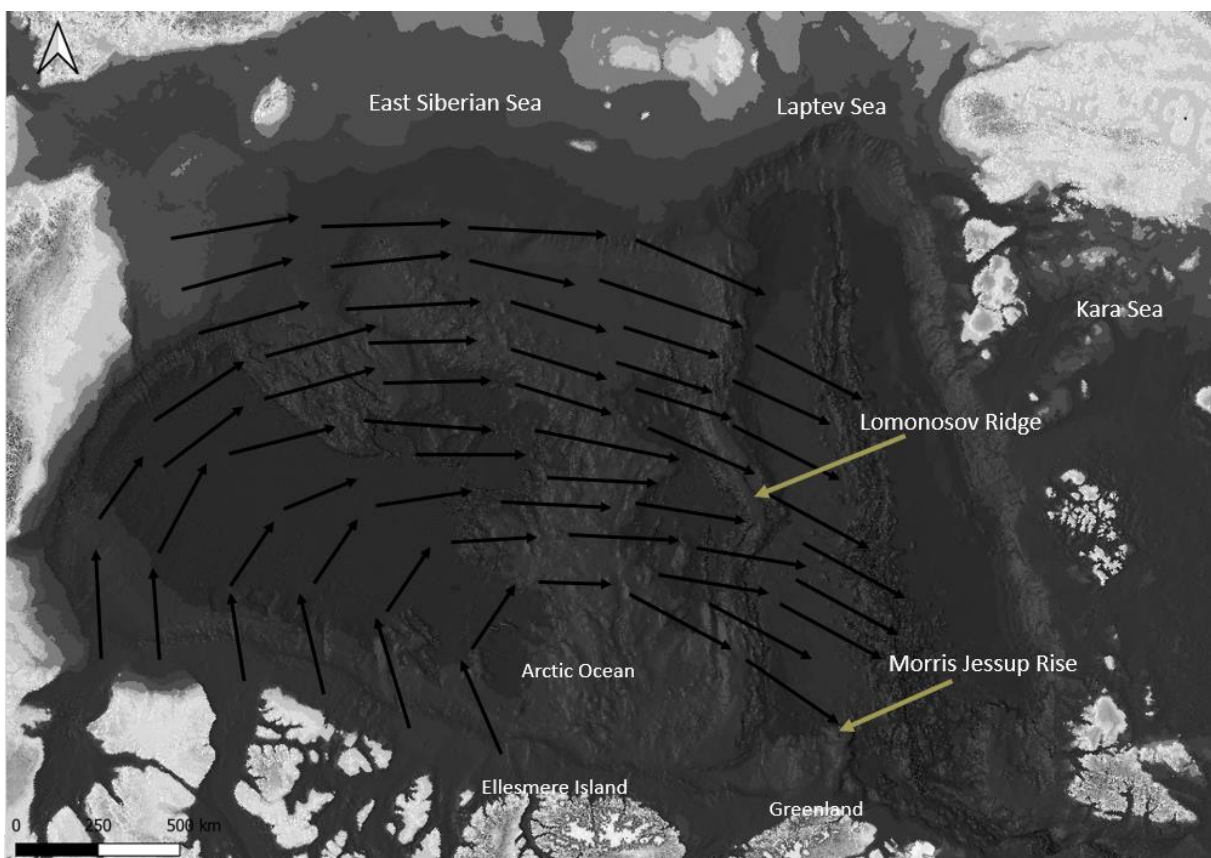


**Figure 28:** The suggested sea ice movement from *Bischof and Darby (1997)* were the sea ice moves to the west at first but then turns to the east towards the Lomonosov Ridge and Morris Jessup Rise.

## 7.2 The sub-ice bedrock of northern Greenland

Directly determining the bedrock geology beneath the Greenland Ice Sheet is difficult. However, a sub-ice geology map of Greenland exists, and has been compiled using results from drilling through the ice, identification of glacial erratics, and geophysical methods (*Dawes, 2009*). The most inland part of northern Greenland contains the Precambrian shield. Further north, around Petermann Fjord, layers of porphyries (rock types with large crystals like granite and gabbro) and redbeds are found. These redbeds generally consist of sandstones and mudstones (*figure 29A*). Areas around the Victoria Fjord also contain old archean rocks. In the eastern part of Greenland, the sub-ice bedrock is heavily

made up of basins containing basalts.

Since all the glaciers in the northern Greenland coast are basically flowing over the Franklinian Basin they should all generally erode the same materials. A slight distinction is that the sandstone and mudstones of the Franklinian Basin are not directly outcropping in front of Petermann, which is the reason for high carbonate content in that area. However, the sub-ice geology suggests that the Lincoln Sea area might contain different rock types than the Petermann area (like the archaic orthogneisses which is coming from below the south end of the Victoria Fjord, *figure 29A*) The basalts that exist in the eastern Greenland were not found in any of the Ryder 2019 samples. This is consistent with the fact that the basins containing basalt are not connected to the Lincoln Sea with present or past ice flow directions. However, there are possibilities that basalt clasts could be found in samples from the Fram Strait since major ice streams are heading towards Fram Strait from the coastal areas containing basalts (*figure 29A*).

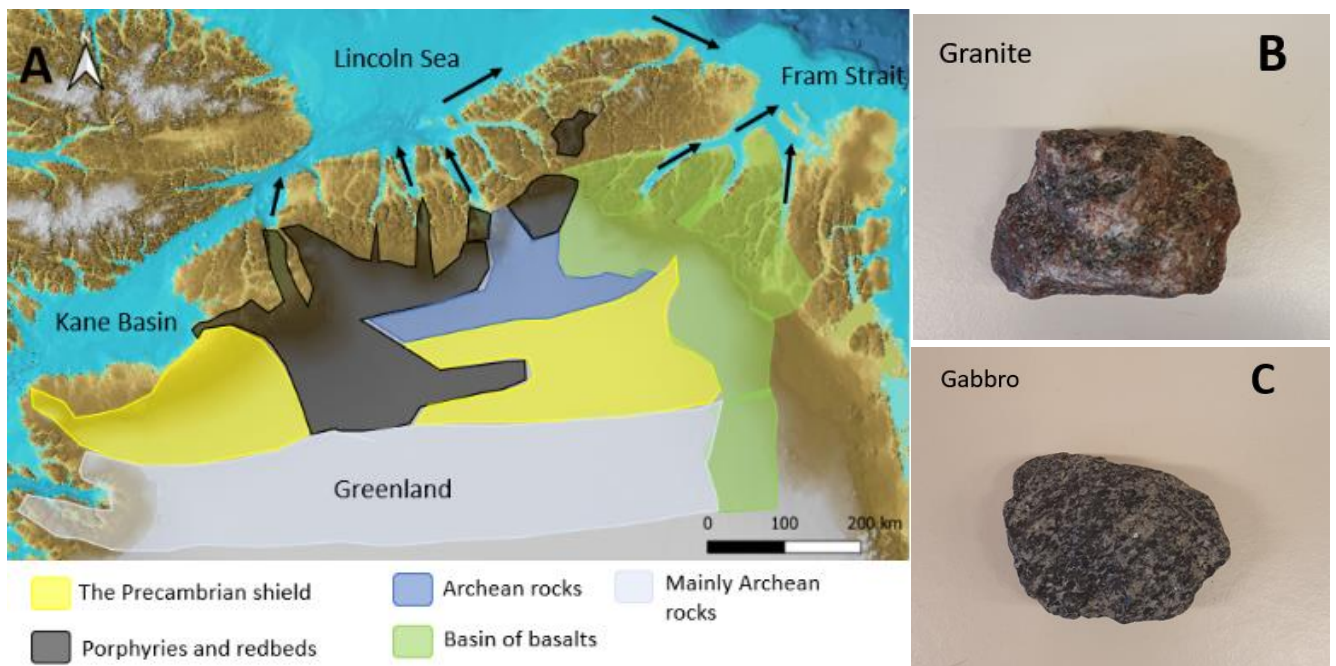


**Figure 29:** The different rock types found under the inland ice (map data from Dawes, 2009) (29A). Typical porphyries of granite (29B) and gabbro (29C) from the northern Greenland samples are also shown.

The granite and gabbro clasts (*figure 29B and figure 29C*) were abundant in Petermann Fjord and the Sherard Osborn Fjord which is consistent with the proposed sub-ice geology in these regions. The larger igneous clasts (>4mm) generally also contain large crystals that indicate porphyries, just like the ones in the bedrock beneath the ice. The sandstone and mudstone below the ice could also have been transported since most samples also contain quite a lot (22-28% for the mudstone and 10-12% for the sandstone) of these rock types. However, since the bedrock on the surface also contains a lot of sedimentary rock types like sandstone and mudstone, it is not really possible to determine if the sedimentary clasts in the Ryder 2019 samples are the same type as the ones in the bedrock below the ice. Further research is most likely needed. Since the sub-ice bedrock does not generally contain any amphibolite and carbonates in the northern Greenland, it is a further proof that the clasts should come from bedrock lithologies outcropping today in northern Greenland.

### 7.3 Comparing clast compositions

The samples from the *Phillips and Grantz (2001)* study show a wide range of variability from across the Arctic. By using a wide distribution of samples from across the Arctic, *Phillips and Grantz* defined two broad clast suites – the Amerasian and Eurasian suites. The Amerasian suite is generally extremely abundant in carbonate like limestone and dolomite, but also contains some mudstone/sandstone and minor parts of igneous -and metamorphic rocks and also a little bit of coal and chert. The Eurasian suite is however, remarkably abundant in mudstone and sandstone instead. The Eurasian clast suite does almost not contain any carbonate and only contains minor amounts of igneous and metamorphic rock. This clast suite also contains a large contribution of coal and chert.

If the northern Greenland samples were similar to the Eurasian clast suite it is likely that clasts were deposited by icebergs trapped in the Transpolar Drift. Icebergs traveling from the Eurasian Basin and in the Transpolar Drift could deposit IRD on the Lomonosov Ridge and Morris Jessup Rise. This material may even have had a local source, as the icebergs may have eroded shallower portions of the Lomonosov Ridge (*Kristoffersen et al 2004*). If the northern Greenland samples were similar to the Amerasian suite, they would likely have been deposited by icebergs traveling in the Beaufort Gyre. Since the Eurasian suite are heavily abundant in mudstone and sandstone (52%) and not very abundant in carbonates (6%) it is clear that they are not reflected in the northern Greenland samples which has around 39% for mudstone/sandstone and 26% for carbonates (*figure 30*). However, both the northern Greenland samples and the Amerasian suite are extremely abundant in carbonate (26% for the northern Greenland samples and 48% for the Amerasian suite). To evaluate whether the Ryder 2019 samples and the *Phillips and Grantz (2001)* Amerasian suite assemblage were significantly different, a T-test was conducted. This analysis indicates that they are significantly different from each other because the t-value was higher than the t-crit value which means that the “null hypothesis” (which means that something is similar to each other) could be rejected.

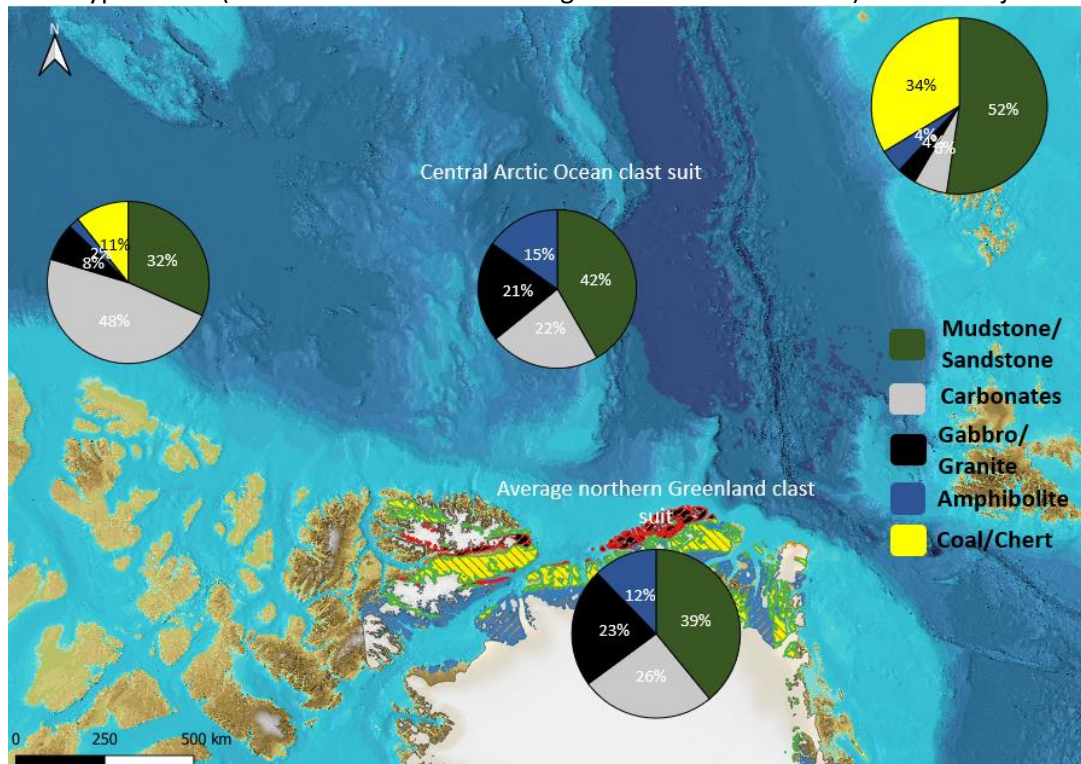


**Figure 30:** Average rock composition for Amerasian, Eurasian, Central Arctic Ocean and the northern Greenland suite used for comparison between the different clast suites (The Amerasian and the Eurasian data are taken from *Phillips and Grantz, 2001*).

An ANOVA analysis was also conducted between the northern Greenland samples and the Central Arctic Oceans samples. The analysis indicates that these two compared assemblages are in fact quite similar to each other, which is a further proof that the ice extended out through iceberg to Lomonosov Ridge and deposited IRD. Compared to the Amerasian suite and the Eurasian suite, the northern Greenland samples and the Central Arctic Ocean samples could be classed as unique for the Arctic Ocean. This suggests that there is potential to use them as a provenance tool in studies of sediments from distal regions of the Arctic.

#### *7.4 Sources of error and future work*

An important source of error is the potential misidentification of rock types. For example, this error occurs because some of the rock types could look quite similar and could therefore be hard to distinguish from each other. One limitation of the current study is the number of available samples. Although 16 samples were washed, only 11 had enough clast material for analyses. The reason why five samples did not really have that many clasts is mainly because the core did not penetrate deep enough into the seafloor to recover a basal diamict.

Based on these results it appears that north Greenland has a unique clast composition compared to previous work on Amerasian and Eurasian basin sediments. Work that could be done for the future is to extend the geographical coverage of samples along the north coast of Greenland and towards the Fram Strait and also south towards Baffin Bay. This could help interpret possible ice flow directions and movements in the region. A major question remains about the direction of ice flow in the Lincoln Sea, where numerous outlet glaciers merged together, and how these fits with the proposed eastward flow of shelf ice, that in principle prevent IRD delivery from northern Greenland into the Central Arctic Ocean. The preliminary analysis in this study, which showed notable similarities between clast compositions on the Lomonosov Ridge and Morris Jessup Rise with those from the Ryder 2019 expedition – suggests that ice from northern Greenland did penetrate into the Central Arctic or the Central Arctic samples were a mixture of the Amerasian, and Eurasian basin suites defined by *Phillips and Grantz (2001)* – where the Beaufort Gyre and the Transpolar Drift converge. Two approaches could help to resolve this, 1) directly dating clast samples, or overlying microfossils rich layers to ensure that the samples are deposited at the same time, under the same paleo-ice conditions, and 2) Extending the number of samples in the Central Arctic Ocean, primarily along the Lomonosov Ridge to establish where the clast assemblage starts to differ from the northern Greenland assemblage but also where the northern Greenland samples starts to reflect the end members defined by *Phillip and Grantz (2001)* even more.

More sophisticated geochemical measurements could also be used to potentially distinguish between similar rock types originating from different areas. For example, using XRF on the samples to distinguish elemental differences in similar rock types or sediments. This was for example done by *Wang et al (2018)* where they used XRF to look at glacial provenance in the Central Arctic Ocean.

## **8. Conclusions**

- Detrital carbonates (limestones and dolomites) make up a substantial proportion of the IRD clasts along the northern Greenland coast.
- Variations in IRD clast provenance from around northern Greenland are consistent with the known past flow directions of glacier ice.
- Carbonate clasts are most abundant in the Petermann Fjord region of the study area which appears to reflect the fact that carbonate sediments of the Franklinian Basin are outcropping directly at the coastline in this region.

- The Ryder samples are likely coming from the currently exposed bedrock lithologies (from the Franklinian Basin) that today lie seaward of the ice margin, and which were overridden and eroded during past glaciations.
- IRD clast assemblages from northern Greenland were similar to those from more distal cores recovered on the southern Lomonosov Ridge and Morris Jessup Rise. This may suggest that icebergs calved from the Ellesmere-Greenland Ice Shelf traveled further into the Central Arctic Ocean.
- Northern Greenland samples and the Central Arctic Ocean samples could be classed as unique for the Arctic Ocean, which means that they can potentially be used as a provenance tool in studies of sediments from distal regions.
- Further work is needed to resolve how the existence of the eastward flowing Ellesmere-Greenland Ice Shelf can be reconciled with the similarities of IRD clasts to the south (Ryder 2019 samples) and north (central Arctic Ocean samples) of it.

## 9. Acknowledgement

I would like to give thanks to the following people for the assistance and participation in this master's thesis. Firstly, I will say thank you to my supervisor Matthew O Regan for the assistance and the new knowledge I have gathered. I would also like to say thank you to Joakim Mansfeld and Helen Coxall for assisting me with the rock types analyzes and identification. In these seven months, I have learned a lot about marine – and bedrock geology which I did not know before. I am also grateful that I had the chance to do this project as my master's thesis.

## 10. References

- Batchelor, C.L., Margold, M., Krapp, M., Murton, D.K., Dalton, A.S., Gibbard, P.L., Stokes, C.R., Murton, J.B., & Manica, A. (2019). The configuration of Northern Hemisphere ice sheets through the Quaternary. *Nat Commun*, Volume 10, Page 3713.
- Bischof, J.F., & Darby, D.A. (1997). Mid- to Late Pleistocene Ice Drift in the Western Arctic Ocean: Evidence for a Different Circulation in the Past. *Science*, Volume 277, Issue 5322, Pages 74-78.
- Blake Jr, W. (1970). Studies of glacial history in Arctic Canada. I. Pumice, radiocarbon dates, and differential postglacial uplift in the eastern Queen Elizabeth Islands. *Canadian Journal of Earth Sciences*, Volume 7(2), Pages 634-664.
- Blake Jr, W., Boucherle, M. M., Fredskild, B., Jannsens, J. A., & Smol, J.P. (1992). The geomorphological setting, glacial history, and Holocene development of Kap Inglefield SØ, Inglefield Land, North-West Greenland. *Geoscience*, Volume 27, Pages 1-42.
- Boucsein, B., Knies, J., & Stein, R. (2002). Organic matter deposition along the Kara and Laptev Seas continental margin (eastern Arctic Ocean) during last deglaciation and Holocene: evidence from organic-geochemical and petrographical data. *Marine Geology*, Volume 183, Issues 1–4, Pages 67-87.
- Box, J.E., & Decker, D.T. (2011). Greenland marine-terminating glacier area changes: 2000–2010. *Ann. Glaciol*, Volume 52, Pages 91–98.
- Bryant, I.D., & Smith, M.P. (1990). A composite tectonic-eustatic origin for shelf sandstones at the Cambrian-Ordovician boundary in North Greenland. *Journal of the Geological Society*, Volume 147, Pages 795-809.
- Butt, F.A., Drange, H., Elverhøi, A., Otterå, O.H., & Solheim, A. (2002). Modelling Late Cenozoic isostatic elevation changes in the Barents Sea and their implications for oceanic and climatic regimes: preliminary results, *Quaternary Science Reviews*, Volume 21, Issues 14–15, Pages 1643-1660.

- Caron, M., Montero-Serrano, J.-C., St-Onge, G., & Rochon, A. (2020). Quantifying provenance and transport pathways of Holocene sediments from the north-western Greenland margin. *Palaeoceanography and Paleoclimatology*, Volume 35, Issue 5.
- Condie, K.A. (1981). Archean Greenstone Belts. Development in Precambrian geology 3. Department of geoscience, New Mexico, Volume 3, Page 1.
- Davies, W.E., & Krinsley, D.B. (1962). The recent regimen of the ice cap margin in northern Greenland. *Int. Assoc. Sci. Hydrol. Publ*, Volume 58, Pages 119–130.
- Dawes, P.R. (1986). Glacial erratics on the Arctic Ocean margin of North Greenland: implications for an extensive ice-shelf. *Bull. geol. Soc. Denmark*, Volume 35, Pages 59-69.
- Dawes, P.R. (2009). The bedrock geology under the Inland Ice: the next major challenge for Greenland mapping. *Geological Survey of Denmark and Greenland Bulletin*, Volume 17, Pages 57–60.
- Donn, W., & Ewing, M. (1966). A Theory of Ice Ages III. *Science*, Volume 152(3730), Pages 1706-1712.
- Dyke, A.S., & Prest, V.K. (1987). Late Wisconsinan and Holocene History of the Laurentide Ice Sheet. *Géographie physique et Quaternaire*, Volume 41(2), Pages 237–263.
- Dyke, A.S., Andrews, J.T., & Miller, G.H. (1982). QUATERNARY GEOLOGY OF CUMBERLAND PENINSULA, BAFFIN ISLAND, DISTRICT OF FRANKLIN. Geological Survey of Canada, Pages 2-32.
- Dyke, A.S., Andrews, J.T., Clark, P.U., England, J.H., Miller, G.H., Shaw, J., & Veillette, J.J. (2002). The Laurentide and Innuitian ice sheets during the Last Glacial Maximum, *Quaternary Science Reviews*, Volume 21, Issues 1–3, Pages 9-31.
- Embry, A., & Beauchamp, B. (2008). Chapter 13 Sverdrup Basin, *Sedimentary Basins of the World*, Elsevier, Volume 5, Pages 451-471.
- England, J. (1976). Late quaternary glaciation of the Eastern Queen Elizabeth Islands, N.W.T., Canada: Alternative models. *Quaternary Research*, Volume 6, Issue 2, Pages 185-202.
- England, J. (1999). Coalescent Greenland and Innuitian ice during the Last Glacial Maximum: Revising the Quaternary of the Canadian High Arctic. *Quaternary Science Reviews*, Volume 18, Issue 3, Pages 421–426.
- England, J., & Bradley, R.S. (1978). Past Glacial Activity in the Canadian High Arctic. *Science*, Volume 200, Issue 4339, Pages 265-270.
- England, J., Atkinson, N., Bednarski, J., Dyke, A.S., Hodgson, D.A., & Cofaigh, C.Ó. (2006). The Innuitian Ice Sheet: configuration, dynamics and chronology. *Quaternary Science Reviews*, Volume 25, Issues 7–8, Pages 689-703.
- Evans, J., O’Cofaigh, C., Dowdeswell, J.A. & Wadhams, P. (2009). Marine geophysical evidence for former expansion and flow of the Greenland Ice Sheet across the north-east Greenland continental shelf. *J. Quaternary Sci*, Volume 24, Pages 279–293.
- Fagel, N., Not, C., Gueibe, J., Mattielli, N., & Bazhenova, E. (2014). Late Quaternary evolution of sediment provenances in the Central Arctic Ocean: mineral assemblage, trace element composition and Nd and Pb isotope fingerprints of detrital fraction from the Northern Mendeleev Ridge. *Quaternary Science Reviews*, Volume 92, Pages 140-154.
- Friderichsen, I.D., Higgins, A.K., Hurst, I.M., Federsen, S.A.S., Soper, N.J., & Surlyk, F. (1982). Lithostratigraphic framework of the Upper Proterozoic and Lower Palaeozoic deep water clastic deposits of North Greenland. *GEOL, Survey of Greenland*, Volume 107, Pages 1-20.
- Funder, S., & Larsen, O. (1982). Implications of volcanic erratics in Quaternary deposits of North Greenland. *Bulletin of the Geological Society of Denmark*, Volume 31, Pages 57-61.
- Funder, S., & Hansen, L. (1996). The Greenland ice sheet-- a model for its culmination and decay during and after the last glacial maximum. *Bulletin of the Geological Society of Denmark*, Volume 42, Pages 137-152.
- Funder, S., Jennings, A.E., & Kelly, M. (2004). Middle and late Quaternary glacial limits in Greenland. In: Ehlers, J., Gibbard, P.L. (Eds.), *Quaternary Glaciations-Extent and Chronology. Part II. North America. Developments in Quaternary Science*, Volume 2b, Pages 425-430.

- Funder, S., Kjellerup Kjeldsen, K., Kjær, K.H., & O’Cofaigh, C. (2011). The Greenland Ice Sheet During the Past 300,000 Years: A Review. *Developments in Quaternary Sciences*, Elsevier, Volume 15, Pages 699-713.
- Hansen, B.T., Kalsbeek, F., & Holm, P.M. (1987). Archaean age and Proterozoic metamorphic overprinting of the crystalline basement at Victoria Fjord, North Greenland. - *Rapport Gronlands Geologiske Undersogelse*, Volume 133, Pages 159- 168.
- Harrison, J.C., St-Onge, M.R., Petrov, O., Strelnikov, S., Lopatin, B., Wilson, F., Tella, S., Paul, D., Lynds, T., Shokalsky, S., Hults, C., Bergman, S., Jepsen, H.F., & Solli, A. (2008). Geological map of the Arctic, Geological Survey of Canada, Open File 5816.
- Henriksen, N., & Higgins, A.K. (2000). Early Palaeozoic Basin Development of North Greenland - Part of the Franklinian Basin, *Polarforschung*, Bremerhaven, Alfred Wegener Institute for Polar and Marine Research & German Society of Polar Research, Volume 68, Pages 131-140.
- Henriksen, N., Higgins, A., Kalsbeek, F., & Pulvertaft, T.C.R. (2009). Greenland from Archaean to Quaternary. Descriptive text to the 1995 Geological map of Greenland, 1:2 500 000. 2nd edition. *GEUS Bulletin*, Volume 18, Pages 1-126.
- Higgins, A.K., & Soper, N.J. (1985). Cambrian – Lower Silurian slope and Basin stratigraphy between northern Nyeboe Land and western Amundsen Land, North Greenland. *Rapp. - Gronl. Geol. Unders.*, Volume 126, Pages 79-86.
- Higgins, A.K. (1989). North Greenland ice islands. *Polar Rec*, Volume 25, Pages 207–212.
- Higgins, A.K., Peel, J.S., S nderho1m, M., Ineson, J.R., & Surlyk, F. (1991A). Lower Paleozoic Franklinian Basin of North Greenland. *Groenlands Geologiske Undersoegelse, Bulletin; (Denmark)*, Volume 160, Pages 71-139.
- Higgins, A.K. (1991B). North Greenland Glacier Velocities and Calf Ice Production. Bremerhaven: Alfred Wegener Institute for Polar and Marine Research & German Society of Polar Research, Volume 60, pages 1-23.
- Hill, E.A., Carr, J.R., & Stokes, C.R. (2017). A Review of Recent Changes in Major Marine-Terminating Outlet Glaciers in Northern Greenland. *Frontiers in Earth Science*, Volume 4, Article 111.
- Hurst, J.M., McKerrow, W.S., Soper, N.J., & Surlyk, F. (1983). The relationship between Caledonian nappe tectonics and Silurian turbidite deposition in North Greenland. - *J. Geol. Soc. Lond.*, Volume 140, Pages 123-132.
- Ineson, J., & Surlyk, F. (1995). Carbonate slope aprons in the Cambrian of North Greenland: geometry, stratal patterns and facies. *Atlas of Deep Water Environments*. Springer, Dordrecht, Pages 56-62.
- Jakobsson, M., Polyak, L., Edwards, M., Kleman, J., & Coakley, B. (2008). Glacial geomorphology of the Central Arctic Ocean: the Chukchi Borderland and the Lomonosov Ridge. *Earth surfaces processes and landforms*, Volume 33, Pages 526-545.
- Jakobsson, M., Andreassen, K., R n Bjarnad ttir, L., Dove, D., Dowdeswell, J., England, J., Funder, S., Hogan, K., Ing lfsson, O., Jennings, A., Krog Larsen, N., Kirchner, N., Landvik, J., Mayer, L., Mikkelsen, N., M ller, P., Niessen, F., Nilsson, J., O’Regan, M., Polyak, L., N rgaard-Pedersen, N., & Stein, R. (2014). Arctic Ocean glacial history. *Quaternary Science Reviews*, Volume 92, Pages 40-67.
- Jakobsson, M., Hogan, K.A., Mayer, L.A., Mix, A., Jennings, A., Stoner, J., Eriksson, B., Jerram, K., Mohammad, R., Pearce, C., Reilly, B., & Stranne, C. (2018). The Holocene retreat dynamics and stability of Petermann Glacier in northwest Greenland, *Nat. Commun*, Volume 9(1), Article 2104.
- Jakobsson, M., Mayer, L., Farrell, J., & Ryder 2019 Scientific Party. (2019). EXPEDITION REPORT SWEDARCTIC Ryder 2019. Swedish polar research secretariat, Page 17.
- Jakobsson, M., Mayer, L.A., Bringensparr, C., Castro, C.F., Mohammad, R., Johnson, P., Ketter, T., Accettella, D., Amblas, D., An, L., Arndt, J.E., Canals, M., Casamor, J.L., Chauch , N., Coakley, B., Danielson, S., Demarte, M., Dickson, M-L., Dorschel, B., Dowdeswell, J.A., Dreutter, S., Fremand, A.C., Gallant, D., Hall, J.K., Hehemann, L., Hodnesdal, H., Hong, J., Ivaldi, R., Kane, E., Klaucke, I., Krawczyk, D.W., Kristoffersen, Y., Kuipers, B.R., Millan, R., Masetti, G., Morlighem, M., Noormets, R., Prescott, M.M., Rebesco, M., Rignot, E., Semiletov, I., Tate, A.J., Travaglini, P.,

- Velicogna, I., Weatherall, P., Weinrebe, W., Willis, J.K., Wood, M., Zarayskaya, Y., Zhang, T., Zimmermann, M., & Zinglensen, K.B. (2020). The International Bathymetric Chart of the Arctic Ocean Version 4.0. *Sci Data*, Volume 7, Article 176.
- Jepsen, H.F., & Kalsbeek, F., (2000). Precambrian Evolution of North and North-East Greenland: Crystalline Basement and Sedimentary Basins. *Polarforschung*, Volume 68, Pages 153-160.
- Johannessen, O. M., Babiker, M., & Miles, M.W. (2013). Unprecedented retreat in a 50-year observational record for Petermann Glacier, North Greenland. *Atmos. Oceanic Sci. Lett.*, Volume 6, Pages 259–265.
- Joughin, I., Fahnestock, M., Kwok, R., Gogineni, P., & Allen, C. (1999). Ice flow of Humboldt, Petermann and Ryder Gletscher, northern Greenland. *J. Glaciol.*, Volume 45, Pages 231–241.
- Kleiber, H.P., Knies, J., & Niessen, F. (2000). The Late Weichselian glaciation of the Franz Victoria Trough, northern Barents Sea: ice sheet extent and timing. *Marine Geology*, Volume 168, Issues 1–4, Pages 25-44.
- Knies, J., Matthiessen, J., Vogt, C., Sverre Laberg, J., Hjelstuen, B., Smelror, M., Larsen, E., Andreassen, K., Eidvin, T., & Vorren, T.O. (2009). The Plio-Pleistocene glaciation of the Barents Sea–Svalbard region: a new model based on revised chronostratigraphy. *Quaternary Science Reviews*, Volume 28, Issues 9–10, Pages 812-829.
- Koch, L. (1923). Preliminary report upon the geology of Peary land, Arctic Greenland. *American Journal of Science* 5, Pages 190-199.
- Korstgard, J.A., & Nielsen, O.B. (1989). Provenance of dropstones in Baffin Bay and Labrador Sea, Leg 105. *Proc. Ocean Drill. Program, Sci. Results*, Volume 105 (eds S. P. Srivastava et al.), Pages 65-Q17 69.
- Kristoffersen, Y., Coakley, B., Jokat, W., Edwards, M., Brekke, H., & Gjengedal, J. (2004). Seabed erosion on the Lomonosov Ridge, central Arctic Ocean: A tale of deep draft icebergs in the Eurasia Basin and the influence of Atlantic water inflow on iceberg motion?. *Paleoceanography*, Volume 19, Issue 3.
- Larsen, P.H., & Escher, J.C. (1987): Additions to the lithostratigraphy of the Peary Land Group (Silurian) in western and central North Greenland. - *Rapp. Gronlands Geol. Unders*, Volume 133, Pages 65–80.
- Larsen, N.K., Kjær, K.H., Funder, S., Möller, P., Van der Meer, J.J.M., Schomacker, A., Linge, H., & Darby, D.A. (2010). Late Quaternary glaciation history of northernmost Greenland – Evidence of shelf-based ice. *Quaternary Science Reviews*, Volume 29, Issues 25–26, Pages 3399-3414.
- Morris, S., Peel, J., Higgins, A., Soper, N.J., & Davis, N.C. (1987). Burgess shale-like fauna from the Lower Cambrian of North Greenland. *Nature*, Volume 326, Pages 181–183.
- Niessen, F., Hong, J., Hegewald, A., Matthiessen, J., Stein, R., Hyoungjun, K., Sookwas, K., Jensen, L., Jokat, W., Nam, S., & Kang, S. (2013). Repeated Pleistocene glaciation of the East Siberian continental margin. *Nature Geoscience*, Volume 6, Pages 842–846.
- Ottesen, D., Dowdeswell, J. A., Landvik, J. Y. & Mienert, J. (2007). Dynamics of the Late Weichselian icesheet on Svalbard inferred from high-resolution sea-floor morphology. *Boreas*, Volume 36, Pages 286-306.
- O'Regan, M., Cronin, T., Reilly, B., Alstrup, A. K. O., Gemery, L., Golub, A., Mayer, L., Morlighem, M., Moros, M., Munk, O. L., Nilsson, J., Pearce, C., Detlef, H., Stranne, C., Vermassen, F., West, G., & Jakobsson, M. (2021). The Holocene dynamics of Ryder Glacier and ice tongue in north Greenland. *The Cryosphere*, in review.
- O'Regan, M., Backman, J., Barrientos, N., Cronin, T. M., Gemery, L., Kirchner, N., Mayer, L. A., Nilsson, J., Noormets, R., Pearce, C., Semiletov, I., Stranne, C., & Jakobsson, M. (2017). The De Long Trough: a newly discovered glacial trough on the East Siberian continental margin. *Clim. Past*, Volume 13, Pages 1269-1284.
- Ottesen, D., Dowdeswell, J. A., Landvik, J. Y. & Mienert, J. (2007). Dynamics of the Late Weichselian icesheet on Svalbard inferred from high-resolution sea-floor morphology. *Boreas*, Volume 36, Pages 286-306.

- Peck, V.L., Hall, I.R., Zahn, R., Grousset, F., Hemming, S.R., & Scourse, I.R. (2007). The relationship of Heinrich events and their European precursors over the past 60ka BP: a multi-proxy ice-rafted debris provenance study in the Northeast Atlantic. *Quaternary Science Reviews*, Volume 26, Issues 7–8, Pages 862-875.
- Peel, J.S., & Sønderholm, M. (1991). Sedimentary Basins of North Greenland. *Bull. Grønlands geol. Unders*, Volume 160, Page 164.
- Perovich, D., Meier, W., Tschudi, M., Hendricks, S., Petty, A.A., Divine, D., Farrell, S., Gerland, S., Haas, C., Kaleschke, L., Pavlova, O., Ricker, R., Tian-Kunze, X., Webster, M., & Wood, K. (2020). Sea Ice. NOAA Arctic Report Card 2020, Pages 1-10.
- Phillips, R.L., & Grantz, A. (2001). Regional variations in provenance and abundance of ice-rafted clasts in Arctic Ocean sediments: implications for the configuration of late Quaternary oceanic and atmospheric circulation in the Arctic. *Marine Geology*, Volume 172, Pages 91-115.
- Polyak, L., Bischof, J., Ortiz, J.D., Darby, D.A., Channell, J.E.T., Xuan, C., Kaufman, D.S., Løvlie, R., Schneider, D.A., Eberl, D.D., Adler, R.E., & Council, E.A. (2009). Late Quaternary stratigraphy and sedimentation patterns in the western Arctic Ocean, *Global and Planetary Change*, Volume 68, Issues 1–2, Pages 5-17.
- Rignot, E., Gogineni, S., Joughin, I., & Krabill, W. (2001). Contribution to the glaciology of northern Greenland from satellite radar interferometry. *J. Geophys. Res*, Volume 106, Issue D24, Pages 34007-34019.
- Shu, Q., Wang, Q., Su, J., Li, X., & Qiao, F. (2019). Assessment of the Atlantic water layer in the Arctic Ocean in CMIP5 climate models. *Clim Dyn*, Volume 53, Pages 5279-5291.
- Soper, N.J., & Higgins, A.K. (1987). A shallow detachment beneath the North Greenland fold belt: implications for sedimentation and tectonics. - *Geol. Mag*, Volume 124(5), Pages 441-450.
- Stokes, C.R., Clark, C.D., Darby, D.A., & Hodgson, D.A. (2005). Late Pleistocene ice export events into the Arctic Ocean from the M'Clure Strait Ice Stream, Canadian Arctic Archipelago, *Global and Planetary Change*, Volume 49, Issues 3–4, Pages 139-162.
- Surlyk, F., & Hurst, J.M. (1984). The evolution of the early Paleozoic deep-water Basin of North Greenland. *GSA Bulletin*, Volume 95 (2), Pages 131–154.
- Surlyk, F., & Ineson, J.R. (1987). Aspects of Franklinian shelf, slope and trough evolution and stratigraphy in North Greenland. - *Rapp. Grønlands Geol. Unders*, Volume 133, Pages 41-58.
- Thomas, R., Frederick, E., Krabill, W., Manizade, S., & Martin, C. (2009). Recent changes on Greenland outlet glaciers. *J. Glaciol*, Volume 55, Pages 147-162.
- Trettin, H.P. (1991). Geology of the Innuitian Orogen and Arctic Platform of Canada and Greenland. - *Geol. Surv. Canada, Geology of Canada*, Volume 3, Page 570.
- Trettin, H.P. (2011). Pearya: a composite terrane with Caledonian affinities in northern Ellesmere Island. *Canadian Journal of Earth Sciences*, Volume 24. Pages 224-245.
- Wang, R., Polyak, L., Xiao, W., Wu, L., Zhang, T., Sun, Y., & Xu, X. (2018). Late-Middle Quaternary lithostratigraphy and sedimentation patterns on the Alpha Ridge, central Arctic Ocean: Implications for Arctic climate variability on orbital time scales. *Quaternary Science Reviews*, Volume 181, Pages 93-108.
- Wetterich, S., Rudaya, N., Tumskey, V., Andreev, A.A., Opel, T., Schirmermeister, L., & Meyer, H. (2011). Last Glacial Maximum records in permafrost of the East Siberian Arctic. *Quaternary Science Reviews*, Volume 30, Issues 21-22, Pages 3139-3151.

## Appendix 1

Counted clasts for each rock type of the northern Greenland samples including total clasts for each sample. The fraction size is >4 mm.

| Sample No.       | Mudstone | Sandstone | Carbonate rock | Granite | Gabbro | Amphibolite | Total # |
|------------------|----------|-----------|----------------|---------|--------|-------------|---------|
| Ryder19-21-GC-CC | 5        | 1         | 4              | 1       | 2      | 1           | 14      |
| Ryder19-24-PC-CC | 12       | 2         | 9              | 2       | 4      | 6           | 35      |
| Ryder19-22-GC-CC | 4        | 1         | 3              | 1       | 2      | 0           | 11      |
| Ryder19-23-GC-CC | 7        | 2         | 10             | 3       | 4      | 6           | 32      |
| Ryder19-07-PC-CC | 5        | 0         | 4              | 1       | 1      | 3           | 14      |
| Ryder19-09-PC-CC | 2        | 1         | 3              | 0       | 3      | 0           | 9       |
| Ryder19-08-PC-CC | 2        | 0         | 1              | 2       | 0      | 1           | 6       |
| Ryder19-12-GC-CC | 12       | 1         | 4              | 0       | 0      | 8           | 25      |
| Ryder19-14-GC-CC | 1        | 0         | 0              | 0       | 0      | 1           | 2       |
| Ryder19-11-GC-CC | 1        | 0         | 0              | 0       | 0      | 0           | 1       |
| Ryder19-13-GC-CC | 1        | 0         | 0              | 0       | 0      | 1           | 2       |
| Ryder19-15-GC-CC | 1        | 0         | 0              | 0       | 0      | 0           | 1       |
| Ryder19-01-GC-CC | 2        | 1         | 3              | 1       | 1      | 2           | 10      |
| Ryder19-16-PC-CC | 6        | 2         | 5              | 1       | 1      | 3           | 18      |
| Ryder19-10-GC-CC | 1        | 0         | 0              | 0       | 0      | 0           | 1       |
| Ryder19-02-GC-CC | 0        | 0         | 0              | 0       | 0      | 1           | 1       |

## Appendix 2

The amount of counted clasts from some of the samples of the legacy dataset of *Phillips and Grantz* from 2001.

